



UNIVERSIDADE DA BEIRA INTERIOR
Engenharia

**Minimum Variance Lateral-Directional Control of a
Bank-to-Turn Missile**
*Controlo Latero-direccional de Variância Mínima
de um Míssil BTT*

David Vicente Medroa

Dissertação para obtenção do Grau de Mestre em
Engenharia Aeronáutica
(ciclo de estudos integrado)

Orientador: Professor Doutor Kouamana Bousson

Covilhã, Abril de 2014

Dedication

To my family that has always been there for me especially to my late grand-mother for all her support.

Acknowledgements

The author wishes to express his gratitude to Professor Doutor Kouamana Bousson for all the help, the support, the time spent during this work. The author also wishes to express his gratitude to his family for the support especially to his parents for all the monetary and moral support without whom this would have ever been possible, and also to the friends found along the way.

Resumo

Este trabalho tem como objectivo projectar um controlador de variância mínima para um míssil Bank-To-Turn (BTT) no voo latero-direccional. O BTT é apenas uma das formas de viragem de um míssil, orientando as forças aerodinâmicas normais, com o plano da direcção do comando usando a arfagem e o rolamento mantendo a derrapagem o mais próximo de zero quanto possível. Num primeiro momento é efectuada uma análise do estado da arte e de alguma história de misseis, em seguida é efectuada uma curta análise dos vários métodos em relação ao BTT, outra área que é estudada é a estabilidade de Lyapunov nas suas mais variadas formas mais propriamente no caso discreto e continuo, em seguida é apresentado o método de H-infinito que servira de método de comparação para finalmente ser apresentado o método da variância mínima, sendo a lei de controlo apresentada em seguida e nesse momento é efectuada a análise. Um controlador de variância mínima consiste, na obtenção da variância mínima da função ou funções utilizadas, de modo a obter uma distribuição o mais normal possível facilitando assim o controlo, é também efectuada uma análise com o método do H-infinito para efeitos de comparação.

Palavras-chave

Misseis BTT, método de variância mínima, H-infinito, controlo

Abstract

The objective of this work is to project a minimal variance controller for a Bank-To-Turn (BTT) missile on the lateral-directional part of the flight. BTT is a way of turning the missile orienting the maximum of normal aerodynamic forces with the plane of the commanded direction using pitch and roll while maintaining a zero sideslip angle. In the first part of this work a brief history and state of the art are made, then the BTT navigation is briefly compared to others, then the BTT navigation is explained. After the introduction the Lyapunov stability is explained in both continuous and discrete, the H-infinity method is now presented then the minimum variance method is described, then the control law is presented, then the analysis is made using Matlab. The objective of the controller is to minimize the variance of the variance of the function or functions used in order to have a smother curve of points and therefore the control is easier, a comparison is made between the methods.

Keywords

BTT missile, guidance, H-infinity, Minimal variance control

Table of Contents

1 Introduction	1
1.1 Generalities about Missiles	1
1.2 Missile definition and history	1
1.3 Bank-To-Turn Versus Skid-To-Turn	4
1.4 Justification of BTT use	5
1.5 Limitation of BTT use	8
1.6 Controller types	8
2 Minimum variance control	15
3 Application	17
3.1 Missile flight Model	17
3.2 Model linearization and Model	18
3.3 Minimum variance controller design	21
3.4 H-infinity Controller design	29
3.5 Comparison	36
4 Conclusion	43
5 References	45
6 Annex A Publication	47

List of Figures

Figure 1.1 -Missile trajectory

Figure 1.2 -Control and guidance schema of a missile

Figure 1.3 -Proportional navigation schema

Figure 1.4 - BTT body rate coupling system

Figure 3.1- Variation of angle of attack α and sideslip angle β with time for the conditions $\alpha = 10^\circ, \beta = 2^\circ, p = q = r = 0, \delta_p = 10^\circ, \delta_q = 20^\circ$

Figure 3.2- Variation of the roll p , the pitch q and the yaw r with time for the conditions $\alpha = 10^\circ, \beta = 2^\circ, p = q = r = 0, \delta_p = 10^\circ, \delta_q = 20^\circ$

Figure 3.3- Variation of the roll controller δ_p , the pitch controller δ_q and the yaw controller δ_r with time for the conditions $\alpha = 10^\circ, \beta = 2^\circ, p = q = r = 0, \delta_p = 10^\circ, \delta_q = 20^\circ$

Figure 3.4- Variation of angle of attack α and the sideslip angle β with time for the conditions $\alpha = 1^\circ, \beta = 0.2^\circ, p = q = r = -50, \delta_p = 10^\circ, \delta_q = 20^\circ, \delta_r = 8^\circ$

Figure 3.5- Variation of roll p , pitch q and yaw r with time for the conditions $\alpha = 1^\circ, \beta = 0.2^\circ, p = q = r = -50, \delta_p = 10^\circ, \delta_q = 20^\circ, \delta_r = 8^\circ$

Figure 3.6- Variation of roll controller angle δ_p , pitch controller angle δ_q and yaw controller angle δ_r with time for the conditions $\alpha = 1^\circ, \beta = 0.2^\circ, p = q = r = -50, \delta_p = 10^\circ, \delta_q = 20^\circ, \delta_r = 8^\circ$

Figure 3.7- Variation of angle of attack α and the sideslip angle β with time for the conditions $\alpha = 10^\circ, \beta = 2^\circ, p = q = r = 0, \delta_p = 10^\circ, \delta_q = 20^\circ$

Figure 3.8- Variation of the roll p , the pitch q and the yaw r with time for the conditions $\alpha = 10^\circ, \beta = 2^\circ, p = q = r = 0, \delta_p = 10^\circ, \delta_q = 20^\circ$

Figure 3.9- Variation of the roll controller angle δ_p , the pitch controller angle δ_q and the yaw controller angle δ_r with time for the conditions $\alpha = 10^\circ, \beta = 2^\circ, p = q = r = 0, \delta_p = 10^\circ, \delta_q = 20^\circ$

Figure 3.10- Variation of angle of attack α and sideslip angle β with time for the conditions $\alpha = 10^\circ, \beta = 2^\circ, p = q = r = 0, \delta_p = 10^\circ, \delta_q = 20^\circ$

Figure 3.11- Variation of the roll p , the pitch q and the yaw r with time for the conditions $\alpha = 10^\circ, \beta = 2^\circ, p = q = r = 0, \delta_p = 10^\circ, \delta_q = 20^\circ$

Figure 3.12- Variation of the roll controller δ_p , the pitch controller δ_q and the yaw controller δ_r with time for the conditions $\alpha = 10^\circ, \beta = 2^\circ, p = q = r = 0, \delta_p = 10^\circ, \delta_q = 20^\circ$

Figure 3.13- Variation of angle of attack α and the sideslip angle β with time for the conditions $\alpha = 1^\circ, \beta = 0.2^\circ, p = q = r = -50, \delta_p = 10^\circ, \delta_q = 20^\circ, \delta_r = 8^\circ$

Figure 3.14- Variation of roll p , pitch q and yaw r with time for the conditions $\alpha = 1^\circ, \beta = 0.2^\circ, p = q = r = -50, \delta_p = 10^\circ, \delta_q = 20^\circ, \delta_r = 8^\circ$

Figure 3.15- Variation of roll controller angle δ_p , pitch controller angle δ_q and yaw controller angle δ_r with time for the conditions $\alpha = 1^\circ, \beta = 0.2^\circ, p = q = r = -50, \delta_p = 10^\circ, \delta_q = 20^\circ, \delta_r = 8^\circ$

Figure 3.16- Variation of angle of attack α and the sideslip angle β with time for the conditions $\alpha = 10^\circ, \beta = 2^\circ, p = q = r = 0, \delta_p = 10^\circ, \delta_q = 20^\circ$

Figure 3.17- Variation of the roll p , the pitch q and the yaw r with time for the conditions $\alpha = 10^\circ, \beta = 2^\circ, p = q = r = 0, \delta_p = 10^\circ, \delta_q = 20^\circ$

Figure 3.18- Variation of the roll controller angle δ_p , the pitch controller angle δ_q and the yaw controller angle δ_r with time for the conditions $\alpha = 10^\circ$, $\beta = 2^\circ$, $p = q = r = 0$, $\delta_p = 10^\circ$, $\delta_q = 20^\circ$

Figure 3.19 Comparison between the minimum variance and H infinity methods for the angle of attack alpha and the sideslip angle beta for the conditions given at examples 1 and 5

Figure 3.20 Comparison between the minimum variance and H infinity methods for roll p, pitch q and yaw r for the conditions given at examples 1 and 5

Figure 3.21 Comparison between the minimum variance and H infinity methods for the roll variation δ_p , the pitch variation δ_q and the yaw variation δ_r for the conditions given at examples 1 and 5

Figure 3.22 Comparison between the minimum variance and H infinity methods for the angle of attack alpha and the sideslip angle beta for the conditions given at examples 2 and 6

Figure 3.23 Comparison between the minimum variance and H infinity methods for roll p, pitch q and yaw r for the conditions given at examples 2 and 6

Figure 3.24 Comparison between the minimum variance and H infinity methods for the roll variation δ_p , the pitch variation δ_q and the yaw variation δ_r for the conditions given at examples 2 and 6

Figure 3.25 Comparison between the minimum variance and H infinity methods for the angle of attack alpha and the sideslip angle beta for the conditions given at examples 3 and 7

Figure 3.26 Comparison between the minimum variance and H infinity methods for roll p, pitch q and yaw r for the conditions given at examples 3 and 7

Figure 3.27 Comparison between the minimum variance and H infinity methods for the roll variation δ_p , the pitch variation δ_q and the yaw variation δ_r for the conditions given at examples 3 and 7.

List of Variables

F_x, F_y, F_z = Forces applied to the missile alongside the missile body x, y and z axes respectively

T_x, T_y, T_z = Thrust applied to the missile alongside the missile body x, y and z axes respectively

W_x, W_y, W_z = Weight applied to the missile alongside the missile body x, y and z axes respectively

g = gravitational acceleration

u, v, w = speed components alongside the missile body x, y and z axes respectively

p = roll

q = pitch

r = yaw

C_l, C_m, C_n = aerodynamic moment coefficients about body x, y and z axes respectively

C_x, C_y, C_z = aerodynamic force coefficients along body x, y, z axes respectively

d = missile reference diameter

$I_{xx}, I_{yy}, I_{zz}, I_{xz}$ = moments of inertia about body

$I_1 - I_5$ = Constants dependent on moments of inertia

K_Q = constant dependent on flight condition

Q = dynamic pressure

S = reference area

u = controller input

α = angle of attack

β = angle of sideslip

δ_p = roll control deflection

δ_q = pitch control deflection

δ_r = yaw control deflection

P = Riccati equation solution

A = System matrix

B = Control matrix

C = Output matrix

D = Disturbance matrix

K = Gain matrix

1. Introduction

1.1. Generalities about Missiles

The defense industry represented in 2012 around 325 billion dollars worldwide, most importantly in North America, Europe, Russia and the People Republic of China. Despite cuts in the defense budgets of the United States and around Europe, this industry is one of the most innovative in the world.

Since the beginning of the missile use, accuracy, a better control during flight among others have always been keys in the missile development, it is possible to see that in accuracy for instance it started in World War II (WW2) with kilometers and now the accuracy can be expressed in millimeters.

As for the control during flight many types of control are used depending of the type of mission and of the missile characteristics, the older one of them is the proportional navigation and decades after both Skid-to-turn (STT) and Bank-to-turn (BTT) appeared and are continuously evolving.

As for guidance, many types of controllers have been used as for instance the Linear Quadratic Regulator (LQR) controller, the H-infinity controller, the Lyapunov controller and the Minimum Variance Controller used in this work.

1.2. Missile Definition and History

1.2.1. Missile definition

A missile is an object made to be fired, thrown, dropped or projected in any other way against a target.

According to range it can be divided in two big categories: the strategic and the tactical missile.

1.2.1.1. Strategic Missile

For this type of missile the range is bigger than 2000 Km, they have a ballistic or semi-ballistic trajectory, they are mostly used against static and strategic targets some examples are the SSBS, MSBS, M20, M4, M45, M51, among others.

1.2.1.2. Tactical Missile

This type of missile usually has a range of less than 500 Km; they can be of various types:

anti-tank- as the HOT or the MILAN,

air-to-air - as the Magic, the Meteor or the sparrow;
air-to-surface- as the AM39 (the Exocet) or the ALARM;
air-to-sea- as the AS15 or the AS30,
surface-to-air- like the Crotale or the Roland;
surface-to-surface - as the MILAN or the Bluewater;
surface-to-sea- as the MM40;
sea-to-sea - as the MM40;
sea-to-air - as the Tomahawk;
sea-to-surface - as the Tomahawk.

1.2.2. Guidance types

As for guidance missiles can be divided in two major types: the command type or homing type.

1.2.1.2.1. Command type

For the command type, the guidance commands are transmitted to the missile by a data link like radio, wire cable or fiber optics and can be of two different types direct or indirect:

In the direct case the detection of the target is made in the missile but the decision and operation are made by the operator(s), the main advantages are the better precision and the need for a good visibility only between the missile and the target, the major inconvenient is the complexity of the system.

For the indirect case both the detection and operation are in the hand of the operator(s), his main inconvenient are the fact that the precision decreases with range, that the visibility need to be optimal between the operator(s) and the target and that it can only be applied to static or slowly moving targets.

1.2.1.2.2. Homing type

The homing missiles are characterized by the ability of the missile to detect, acquire and track a target, various methods can be used.

This guidance can be direct if the missile does everything by itself.

The main advantages are the better precision, the perfect visibility is only needed between the missile and the target, and it is perfectly adapted to fast and mobile targets.

The major inconvenient is the complexity of the system.

In the indirect case the operator gives the missile the missile-target coordinates mainly used in surface-to-air missiles the main inconvenient is the decrease of the precision.

1.2.1.3. Missile trajectory

The typical missile trajectory consists in five phases, represented in fig. 1.1:

Launch- first phase of the trajectory the missile is launched from a platform and suffers a fast acceleration passing to the next phase.

Midcourse guidance- typically it is aimed for the missile to maintain the heading and a constant altitude and the missile is usually blind it usually ends at a rendezvous point.

Detection - In this phase the missile seeker, scans the spectrum looking for the target and then move on to next phase.

Acquisition phase - in this phase the seeker, acquire the target previously detected in this process the missile calculate the angular location of the target and the distance between them obtaining a course initiating the final phase.

Terminal guidance - last phase of the trajectory of the missile phase where given the data from the previous phase the missile will attempt to hit his target.

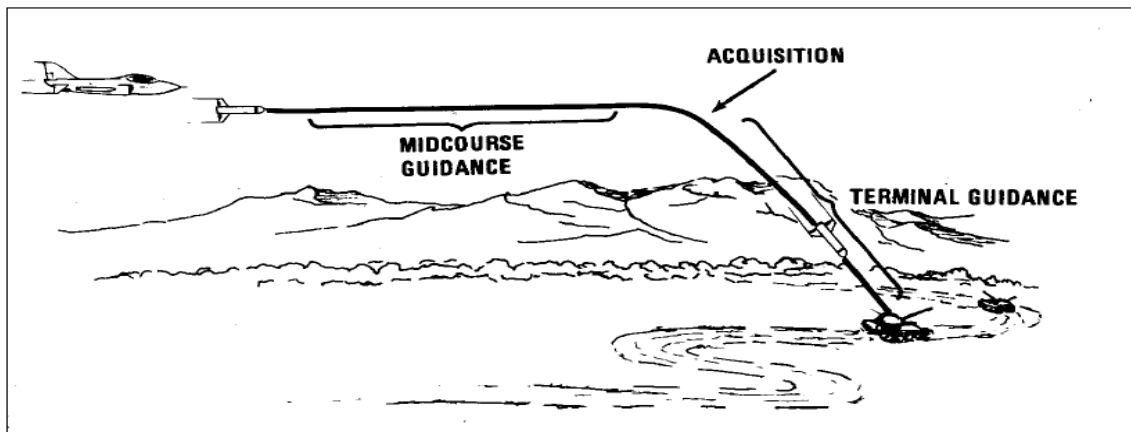


Figure 1.1 missile trajectory

Guidance errors of a tactical missile are greater than the ones of a ballistic, a few of the major errors in the accuracy are: incorrect direction at takeoff (heading error), environmental influences and unpredictable target maneuvers.

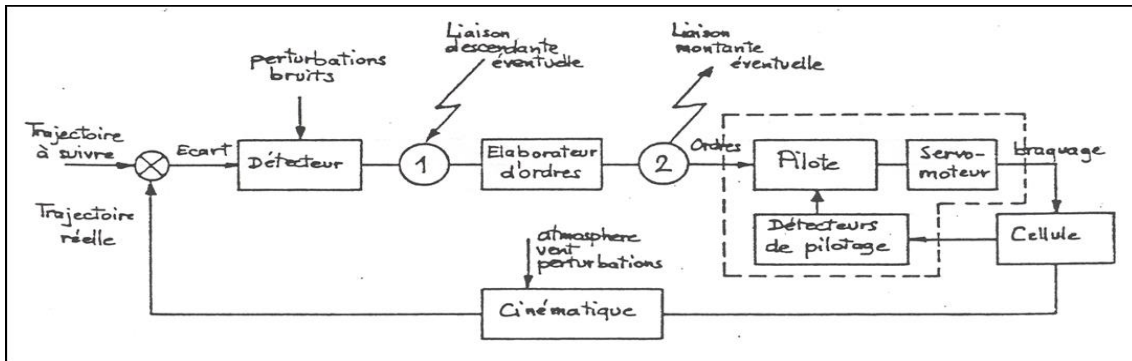


Figure. 1.2 control and guidance schema of a missile

Fig. 1.2 represents the schema of guidance and controls usually used in a missile, the area outside the dashed line represent the control and the area inside represent the guidance.

1.2.2. History

It all started in ancient China in the 13th century spreading to Mongolia, to Russia and the rest of Europe [1].

In 1913 the French engineer René Lorin proposed for patent the ramjet engine thus starting the modern missile history.

In 1931 in Germany the first European flight with a liquid propeller engine was made.

Around 1936 Germany starts a large scale missile program the “Peermünde Project” from which the V-1 and V-2 where born during WW2, simultaneously the USA started various projects one of them being the Razon project in 1943 with its biggest point the development of the atlas intercontinental ballistic missile (ICBM) [1].

Another American project was the Manhattan Project where both European and North American scientists developed the first nuclear leading eventually to the bombing of the two Japanese cities of Hiroshima and Nagasaki.

In 1953 The Soviet Union developed the project R-2 R-5 and R-7 led by the soviet engineer Sergei Korolev, the R-7 is responsible for the launch of the first satellite sputnik-1.

A military example of a missile use is the Falkland war where missiles had for the first time in a regional war a significant importance, especially giving the Exocet a name for itself. The first worldwide large scale use of missiles came in the Persian Gulf War, in which the Iraqis first attacked Israel and Saudi Arabia with SCUD/Al Hussein missiles leading to the international coalition deployment of Patriot missiles, it was also the first time that Tomahawks were used in conflicts [2].

1.3. Bank-To-Turn Versus Skid-To-Turn

First of all let’s define BTT; it is no more than a way of turning a missile orienting, a maximum of aerodynamic normal force, with the plane of the commanded direction using the pitch and roll movement while maintaining a zero sideslip angle.

Before making a brief comparison between BTT and STT it is important to define STT; it is a way of turning a missile where it does not roll to the pretended angle but slide to the desired direction, the sideslip angle control most of the movement.

A brief comparison between BTT and STT will be made in the following categories, guidance performance, guidance logic, autopilot, seeker, body rate coupling, roll yaw aerodynamic coupling, communication antenna, and analysis, using reference [3].

Guidance performance- in STT the maneuvers remain in desired plan and the response time dependent on pitch autopilot while in BTT the Bank maneuver causes airframe to leave desired maneuver plan and the response time depends on pitch and roll autopilot.

Guidance logic- in STT pitch and yaw can be independent while in BTT the bank command is undefined for small pitch accelerations and an additional noise reduction may be required for these cases.

Autopilot - in STT Pitch and yaw systems are identical as opposed to BTT where the turn coordination required if side slip is to be constrained and requires compensation for aerodynamic and kinematic cross coupling.

Seeker - in STT the slew rate requirements determined by stabilization requirements and/or search pattern design and the antenna polarization matched to radiation in opposite, in the BTT case the slew rate capability must be compatible with missile bank motion, low frequencies signal processing requirements may differ from STT, Polarization mismatches decrease antenna gain and may increase random error for semi active systems, polarization changes may alter aim point for active systems against large targets.

Body Rate coupling - in STT the pitch and yaw rates couple into guidance signals and the system may tolerate linear instability while in BTT pitch yaw and roll rates couple into guidance signals BTT systems appear to be more sensitive.

Roll yaw aerodynamic coupling - in STT coupling can limit angle of attack for some orientations as in BTT the system can maintain orientations which minimize coupling.

Communication antenna - in STT the orientation is fixed at all times and in BTT the orientation change as missile banks.

Analysis - in STT the problem can usually be simplified by assuming two independent steering channels and a roll channel in BTT complex coupling requires three dimensional analysis and simulations are required.

1.4. Justification of BTT use

The reason why BTT was used in this work, is due the fact that compared with others like STT he offers a best range for the same amount of fuel, a much larger acceleration in the maneuver plan, a better aerodynamic efficiency and allows to have biggest g forces in at the final part of the flight for this reason it might be used in short, mid and long air to air strikes as well as in air to surface missiles [4].

BTT also have a better maneuverability and can handle a larger rate of rolls.

1.4.1. BTT flight model

After the short comparison between BTT and STT it is time to focus on explaining BTT.

First of all, BTT missiles have like many others airframes six degrees of freedom.

The three forces equations are

$$F_x + T_x + W_x = \frac{W}{g} [\dot{u} + qw - rv] \quad (1.1)$$

$$F_y + T_y + W_y = \frac{W}{g} [\dot{v} + ru - pw] \quad (1.2)$$

$$F_z + T_z + W_z = \frac{W}{g} [\dot{w} - qu + pv] \quad (1.3)$$

where F represents the forces, T the thrust, W the weight, p the roll, q the pitch, r the yaw, u, v and w the axial speeds.

The equations of moments are

$$l = I_{xx} \dot{p} [I_{yy} - I_{zz}] qr + I_{yz} [r^2 - q^2] - I_{xx} [pq + \dot{r}] + I_{xy} [rp - \dot{q}] \quad (1.4)$$

$$m = I_{yy} \dot{q} [-I_{zz} - I_{xx}] rp + I_{xz} [p^2 - r^2] - I_{xy} [qr + \dot{p}] + I_{yz} [pq - \dot{r}] \quad (1.5)$$

$$n = I_{zz} \dot{r} [I_{xx} - I_{yy}] pq + I_{xy} [q^2 - p^2] - I_{yz} [rp + \dot{q}] + I_{xz} [qr - \dot{p}] \quad (1.6)$$

those equations can be written in a matrix form as follow

$$\begin{bmatrix} l \\ m \\ n \end{bmatrix} = J^{-1} \begin{bmatrix} \dot{p} \\ \dot{q} \\ \dot{r} \end{bmatrix} + H(p, q, r) \quad (1.7)$$

were

$$J = \begin{bmatrix} I_{xx} & -I_{xy} & -I_{xz} \\ -I_{xy} & I_{yy} & -I_{yz} \\ -I_{xz} & -I_{yz} & I_{zz} \end{bmatrix} \quad (1.8)$$

and

$$H = \begin{bmatrix} -(I_{yy} - I_{zz})qr + I_{yz}(r^2 - q^2) - I_{xy}pq + I_{xy}rp \\ -(I_{zz} - I_{xx})rp + I_{xz}(p^2 - r^2) - I_{xy}qr + I_{yz}pq \\ -(I_{xx} - I_{yy})pq + I_{xy}(q^2 - p^2) - I_{yz}rp + I_{xz}qr \end{bmatrix} \quad (1.9)$$

with this it is possible to determine nonlinear state equations considering

$$T_x - T_y - T_z = 0 \quad (1.10)$$

for the weights the following equations are obtained

$$W_y = W \cos(\theta) \sin(\varphi) \quad (1.11)$$

And

$$W_z = W \cos(\theta) \cos(\varphi) \quad (1.12)$$

having this in mind

$$F_y = \frac{W}{g} \left(\dot{v} + ru - pw \right) - W_y \quad (1.13)$$

And

$$F_z = \frac{W}{g} \left(\dot{w} - qu + pv \right) - W_z \quad (1.14)$$

the angle of attack and the sideslip angle are given as follow

$$\alpha = \tan^{-1} \left(\frac{w}{u} \right) \quad (1.15)$$

$$\beta = \tan^{-1} \left(\frac{v}{u} \right) \quad (1.16)$$

for small angles the previous equations can be written as follow

$$\alpha = \frac{w}{u} \quad (1.17)$$

$$\beta = \frac{v}{u} \quad (1.18)$$

the total speed of the missile is given by

$$V = \left[(u^2 + v^2 + w^2) \right]^{1/2} \quad (1.19)$$

due to the fact that the most of the time the missile is along the x axis, the following assumptions can be made $u \approx V$ and $\dot{u} \approx 0$, knowing this, the forces equations can be written as follow

$$F_y = \frac{WV}{g} \left(\dot{\beta} + r - p\alpha \right) - W_y \quad (1.20)$$

And

$$F_z = \frac{WV}{g} \left(\dot{\alpha} - q + p\beta \right) - W_z \quad (1.21)$$

[3].

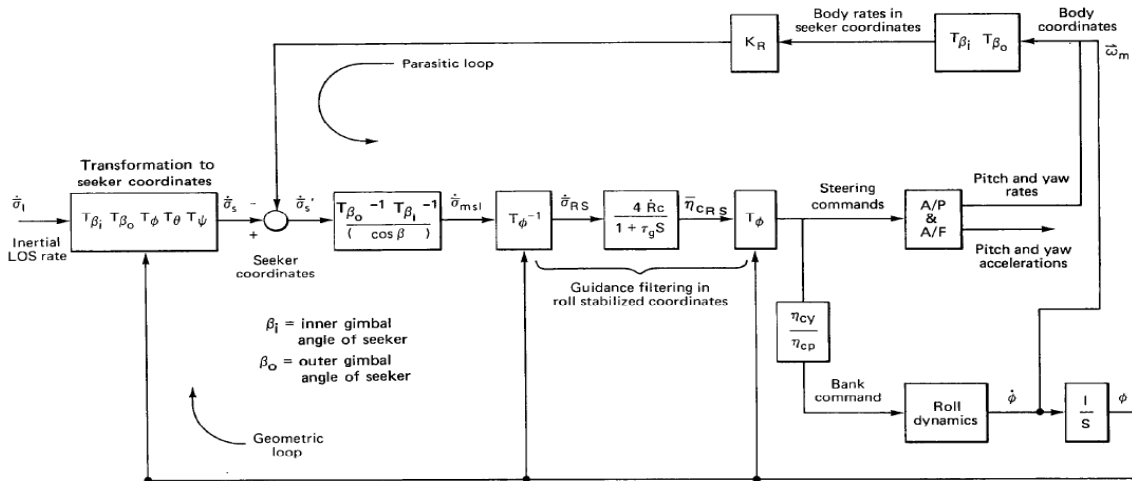


Figure 1.3 BTT body rate coupling system

Fig. 1.3 shown in reference [3] as we can see the line of sight rate is entered in the seeker to help make the seeker coordinates transformations for yaw, roll and pitch and inner and outer gimbal seeker angles, those coordinates are filtered with roll stabilized coordinates, as we can see the fig. 1.3 has two loops, one from the rotation rates ω including $\dot{\phi}$, which is the roll rate, through the matrix, which is the modulation of the body rate perturbations, and a second geometric loop from ϕ , the roll to the transformations. The gain of the first loop is inversely proportional to the pitch acceleration command, η_{CP} since it is in the denominator on the roll command function. For this reason, it is possible to reduce the sensitivity of the loop to body rate coupling by shaping trajectory during terminal homing so that the pitch acceleration is always substantial. The geometric loop is independent of the pitch acceleration This can be observed by linearizing the feedback path ϕ to $\dot{\sigma}_s$. This feedback will have a term proportional to $\dot{\sigma}_s$ which cancels the denominator term in the bank command function. Thus trajectory shaping will not affect the dynamics of the geometric loop.

1.5. Limitations of BTT use

Since BTT uses a high roll rate then one of the biggest limitations will be the cross coupling maneuvers that can create undesired pitch and yaw, and can also generate nonlinearities in linear cases like this one.

Another limitation of BTT use happens in the terminal phase of the flight when a small cross coupling can lead to an increase in the miss distance and in a worst accuracy, in the final part of the flight the BTT response can also be slower than required.

1.6. Controller types

1.6.1. Lyapunov stability

1.6.1.1. Lyapunov stability theorem

If the model is in the real domain and the function $\dot{x} = f(x)$ is continuously differentiable then the rate of change named $\dot{V}(x)$ is given by

$$\dot{V}(x) = \frac{\delta V}{\delta x} f(x) \quad (1.22)$$

called the total or absolute derivative of V .

The derivative along the trajectory of the system given by $\dot{x} = f(x)$ is dependent of its equations since they will be different, if $\phi(t, x)$ is the solution of $\dot{x} = f(x)$

$$\dot{V}(x) = \frac{d}{dt} V(\phi(t, x)) \quad (1.23)$$

If the system is linear then the direct or first method and $x=0$ is an equilibrium point for $\dot{x} = f(x)$ and $D \subset \mathfrak{R}^n$ is invariant and $V : D \rightarrow \mathfrak{R}$ be a continuously differentiable function such that

$$\begin{aligned} V(0) = 0 \quad \text{and} \quad V(x) > 0 \quad \forall x \in D \setminus \{0\} \\ \dot{V}(x) \leq 0 \quad \forall x \in D \end{aligned} \quad (1.24)$$

then, $x = 0$ is a stable equilibrium state. Moreover if

$$\dot{V}(x) < 0 \quad \forall x \in D \setminus \{0\} \quad (1.25)$$

then $x = 0$ is an asymptotically stable equilibrium state.

If $x = 0$ is an equilibrium point for the system let $V : \mathfrak{R}^n \rightarrow \mathfrak{R}$ be a positive definite continuously differentiable function.

If $\dot{V} : \mathfrak{R}^n \rightarrow \mathfrak{R}$ is negative then x is stable; if \dot{V} is negative then x is asymptotically stable.

For a better understanding of the next example the Weierstrass's theorem for extreme values that states that if a real-valued function is continuous in a closed and bounded interval, then the function must have a maximum and minimum at least once in the interval.

Example:

Being $\dot{V} : \mathfrak{R}^n \rightarrow \mathfrak{R}$ is negative given $\varepsilon > 0$ considering the closed ball $\bar{B}(0, \varepsilon)$. Since the boundary $S(0, \varepsilon)$ is compact closed and bounded and V is continuous, V admits a minimum m on $S(0, \varepsilon)$ by Weierstrass's theorem such minimum is positive because V is positive

$$\min_{\{x: \|x\|=\varepsilon\}} V(x) = m > 0 \quad (1.26)$$

since V is continuous, in particular at the origin there exists a positive delta such that

$$x \in B(0, \delta) \Rightarrow |V(x) - V(0)| = V(x) < m \quad (1.27)$$

this delta is the right delta required in the definition of stability so that any trajectory starting from $B(0, \delta)$ never exists $B(0, \varepsilon)$.

1.6.1.2. Instability theorem of Lyapunov

In [5] it is possible to consider autonomous dynamical systems an assuming that $x=0$ is an equilibrium point let $V : D \rightarrow \mathfrak{R}$ have the following properties:

$$(i) \quad V(0) = 0 \tag{1.28}$$

$$(ii) \quad \exists x_0 \in \mathfrak{R}^n \text{ Arbitrarily close to } x=0 \text{ such that } V(x_0) > 0;$$

$$(iii) \quad \dot{V} > 0 \quad \forall \quad x \in U, \text{ where the set } U \text{ is defined as follows:}$$

$$U = \{x \in D : \|x\| \leq e \text{ and } V(x) > 0\} \tag{1.29}$$

under these conditions $x = 0$ is unstable.

Considering the system:

$$\dot{x}_1 = x_2 + x_1(\beta^2 - x_1^2 - x_2^2) \tag{1.30}$$

and

$$\dot{x}_2 = -x_1 + x_2(\beta^2 - x_1^2 - x_2^2) \tag{1.31}$$

the origin of this system is an unstable equilibrium point this result will be verified using Chetaev's result let

$$V(x) = \frac{1}{2}(x_1^2 + x_2^2) \tag{1.32}$$

thus we have that $V(0) = 0$ and moreover

$$V(x) > 0 \quad \forall x \in \mathfrak{R}^2 \neq 0 \tag{1.33}$$

i.e., $\dot{V}(\cdot)$ is positive definite also

$$\dot{V} = (x_1, x_2) f(x) = (x_1^2 + x_2^2)(\beta^2 - x_1^2 - x_2^2) \tag{1.34}$$

defining the set U by

$$U = \{x \in \mathbb{R}^2 : \|x\| \leq \varepsilon, 0 < \varepsilon < \beta\} \quad (1.35)$$

and having that

$$V(x) > 0 \quad \forall x \in U \quad x \neq 0 \quad \text{and} \quad \dot{V} > 0 \quad \forall x \in U \quad x \neq 0 \quad (1.36)$$

thus the origin is unstable by Chetaev result.

1.6.1.3. Lyapunov stability theory for a discrete case

For a discrete system [6], shows that the basic equation is

$$x(k+1) = f(x(k), 0, k) \quad (1.37)$$

the point \bar{x} is an equilibrium point from the time k_0 if

$$f(\bar{x}, 0, k) = \bar{x} \quad \forall k \geq k_0 \quad (1.38)$$

for a linear system stability in a LTI (linear time invariant) case considering a system with a diagonalizable A matrix and $u = 0$ the equilibrium point is at $x = 0$ provided A has no eigenvalue at 1 if this is to happen the every point in the eigenspace is in equilibrium knowing that

$$x(k) = A^k x(0) = V \begin{bmatrix} \lambda_1^k & 0 & 0 \\ 0 & \ddots & 0 \\ 0 & 0 & \lambda_n^k \end{bmatrix} Wx(0) \quad (1.39)$$

for the system to be asymptotically stable

$$|\lambda_i| < 1 \quad \forall i \in \{1, \dots, n\} \quad (1.40)$$

the system is only marginally stable.

All linear quadratic Lyapunov results have discrete time counterpart the discrete time Lyapunov equation is

$$A^T P A - P + Q = 0 \quad (1.41)$$

meaning if

$$x_{t+1} = A x_t \quad (1.42)$$

And

$$V(z) = Z^T P Z \quad (1.43)$$

And

$$\Delta V(Z) = -Z^T Q Z \quad (1.44)$$

where:

1- if $P > 0$ and $Q > 0$ then A is stable (i.e., $|\lambda_1| < 1$)

2- if $P > 0$ and $Q \geq 0$ then all trajectories are bounded (i.e., $|\lambda_i| \leq 1, |\lambda_i| = 1$ only for 1 x1 Jordan block

3- if $P > 0, Q \geq 0$ and (Q,A) is observable then a is stable

4- if $P \leq 0$ and $Q \geq 0$ then A is not stable

The discrete time Lyapunov operator is given by

$$L(P) = A^T P A - P \quad (1.45)$$

L is non-singular if and only if

$$i, j, \lambda_i, \lambda_j \neq 1 \quad (1.46)$$

is the unique solution of Lyapunov equation providing $Q = Q^T$

$$A^T P A - P + Q = 0 \quad (1.47)$$

the discrete-time Lyapunov equation can be solved quickly (i.e., $O(n^3)$) can be used to evaluate infinite sums of quadratic functions.

1.6.2. H- infinity controller

First of all a brief description of the H-infinity theory will now be made, if one considers the following system

$$\begin{aligned} \dot{x} &= Ax + Bu + Dd \\ y &= Cx \end{aligned} \quad (1.48)$$

And a performance output $z(t)$ that satisfies

$$\|z(t)\|^2 = x^T Q x + u^T R u \quad (1.49)$$

For some positive matrices $Q \geq 0$ and $R > 0$. Assuming C has a full row rank.

Considering a L_2 system its gain is said to be bounded or attenuated by γ if

$$\frac{\int_0^{\infty} \|z(t)\|^2 dt}{\int_0^{\infty} \|d(t)\|^2 dt} = \frac{\int_0^{\infty} (x^T Q x + u^T R u) dt}{\int_0^{\infty} (d^T d) dt} \leq \gamma^2 \quad (1.50)$$

It is possible to define a constant output-feedback control as

$$u = -Ky = -Kcx \quad (1.51)$$

It is desired to find a constant output-feedback gain K such that the system is stable.

If one assume that $Q \geq 0$ and (A, \sqrt{Q}) is detectable then the output-feedback is stabilizable with L_2 gain bounded by γ if (A, B) is stabilizable and (A, C) is detectable and there exists matrices K^* and L such that $K^* C = R^{-1}(B^T P + L)$ where $P > 0$, $P^T = P$ is a solution of

$$PA + PA^T + Q + \frac{1}{\gamma^2} PDD^T P - PBR^{-1}B^T P + LR^{-1}L = 0 \quad (1.52)$$

The solution of the H-Infinity Control problem contains Riccati Equations as the following equation

$$A^T P + AP + Q - PBR^{-1}B^T P = 0 \quad (1.53)$$

The stabilizing solution of this equation is given by $P = Riccati(H)$ where H is

$$H = \begin{bmatrix} A & -BR^{-1}B^T \\ -Q & -A^T \end{bmatrix} \quad (1.54)$$

[7]

The main advantage of this controller is the fact that it will reduce or even cancel the noise and the main disadvantages are the fact that it will always oversize the controllers with heavy and difficult computation and a high energy consumption.

1.6.3. Minimum Variance controller

The Minimum variance controller consists in predicting the system in the next used time in order to control the system in the present time and seeks a control that minimizes a determinate performance function that for this work will be given in the next chapter.

The advantages of this type of controllers are simpler to implement and just as fast as other methods offering a good stability for linearized models thus allowing to minimize the cross coupling problem of a latero directional BTT model one of the BTT biggest inconvenient, not compromising speed. Therefore, this is the reason why a minimum variance controller is used in this work.

In the next chapter the minimum variance controller used will be explained and detailed and finally in the third chapter the missile dynamics equations will be given and the analysis will be made.

2. Minimum variance control

In [8] it is possible to see the following linear finite dimensional difference equation

$$y(k+1) = Ay(k) + Bu(k) + c(k) + v(k) \quad (2.1)$$

where $y(k)$ is a n -dimensional output/target vector observed in period k ; $u(k)$ is a m -dimensional input/control vector with $m \leq n$; $c(k)$ is a p -dimensional deterministic input, called exogenous input and is assumed to be known at period k ; $v(k)$ is a serially uncorrelated vector with zero mean and covariance V (white noise).

Assuming that matrix B is injective (full column rank) and that the pair (A, B) is controllable.

Considering the cost functional equation

$$J = E\left\{\left(y(k) - y^*(k)\right)^T P \left(y(k) - y^*(k)\right)\right\} \quad (2.2)$$

where $E\{\}$ denotes the expectation, $y^*(k)$ is a reference value for $y(k)$ and P is symmetric positive definite weighting matrix.

Assuming that the reference trajectory is given by the first order difference equation

$$y^*(k+1) = A^* y^*(k) \quad (2.3)$$

knowing $y^*(0)$ and A^* .

Subtracting equations (2.3) from (2.1) yields

$$e(k+1) = Ae(k) + Bu(k) + x(k) + v(k) \quad (2.4)$$

where

$$e(k) = y(k) - y^*(k) \quad (2.5)$$

And

$$x(k) = (A - A^*)y^*(k) + v(k) \quad (2.6)$$

the optimal control minimizing J subject to the last equation is given by straight forwarding differentiation and equals

$$u(k) = -\left(B^T P B\right)^{-1} B^T P (Ae(k) + x(k)) \quad (2.7)$$

the resulting closed loop system then reads as follows

$$e(k+1) = M[Ae(k) + x(k)] + v(k) = Fe(k) + Mx(k) + v(k) \quad (2.8)$$

And

$$M = I - B(B^T P B)^{-1} B^T P \quad (2.9)$$

A bounded reference trajectory $y^*(.)$ is weakly admissible if the exogenous input sequence $\{e(k)\}$ is bounded and F is stable

Given this the following equation can be written

$$e(k+1) = \sum_{i=0}^k F^i (M_x(k-i) + v(+i)) + F^{k+i} e(0) \quad (2.10)$$

since due to the assumptions on $y^*(.)$ and $e(.), x(.)$ is bounded we have that

$$\|E\{e(k+1)\}\| = \left\| \sum_{i=0}^k F^i M_x(k-i) + F^{k+i} e(0) \right\| \leq \sum_{i=0}^k \|F^i M\| \alpha + \|F^{k+i} e(0)\| \quad (2.11)$$

where

$$\alpha = \sup \|x(k)\| \quad (2.12).$$

Now

$$\sum_{i=0}^k \|F^i M\| \leq \beta < \infty \quad (2.13)$$

if F is stable, in other words all of F eigenvalues must be negatives.

Theorem 1- Let K be any positive definite matrix and let P be the corresponding positive definite solution of the following Riccati equation

$$P = A^T \left\{ P - PB(B^T P B)^{-1} B^T P \right\} A + K \quad (2.14)$$

then the feedback gain F is stable.

Proof - since the pair (A, B) is controllable B is injective and K is positive definite this result follows immediately as a special case from Proposition 3 in [9], in the last mentioned paper it is also proved that under those conditions the Riccati equation possesses a unique positive definite solution. Under the assumption that positive control costs are involved that proof works also in this case since, due to the assumption $B^T K B$ is a positive definite.

Note that the stabilizing weighting matrix P is always positive definite. This propriety is not a prerequisite to obtain a stabilizing Minimum Variance controller. It is shown that in general also semi-positive weighting matrices exist it gives a stabilizing Minimum variance controller.

3. Application

3.1. Missile flight model

Since a BTT missile is nearly symmetrical in the pitch plane, two of the three cross products of inertia (I_{xy}, I_{yz}) are assumed to be zero, with these assumptions the missile dynamics are given as follows:

$$\begin{aligned}
 \dot{\alpha} &= K_Q [-C_x \sin a + C_x \cos \alpha] - \tan \beta (\rho \cos a + r \sin \alpha) + q \\
 \dot{\beta} &= K_Q [C_y \cos \beta - C_x \cos a \sin \beta - C_x \sin \alpha \sin \beta] - r \cos a - p \sin a \\
 \dot{p} &= I_1 pq + I_2 QSdC_l + I_3 QSdC_n \\
 \dot{q} &= \left(\frac{I}{I_{yy}} \right) \left[I_{xz} (r^2 - p^2) + (I_{zz} + I_{xx}) pr + QSdC_m \right] \\
 \dot{r} &= I_4 pq + I_3 QSdC_l + I_5 QSdC_n
 \end{aligned} \tag{3.1}$$

Note that the preceding equations exhibit significant explicit kinematic and inertial coupling and implicit through the aero coefficients. Specifically a BTT missile will develop a large roll rate and angle of attack while maintaining a small sideslip angle.

Therefore, the roll rate will require a large yaw rate to maintain zero sideslip will then be coupled into the pitch plane dynamics, the pitch dynamics also appear in the yaw/roll equations.

The precedent set of equations alongside the inertia moments allow us when integrated obtain the aerodynamic coefficients that will allow us to solve the forces and moment equations shown previously

The controls appear in the aerodynamic force and moment coefficients, which in general are complicated nonlinear functions of both the states and controls.

These are in the form of tabular data and so functional approximations were created by curve fitting the resulting aerodynamic model is as follows

$$\begin{aligned}
 C_x(\alpha) &= C_{x0} + C_{x\alpha} \alpha \\
 C_y(\beta, \delta_r) &= C_{y\beta} \beta + C_{y\delta_r} \delta_r \\
 C_z(\alpha, \delta_q) &= C_{z0} + C_{z\alpha} \alpha + C_{z\delta_q} \delta_q \\
 C_l(\alpha, \beta, \delta_p, \delta_r) &= (a_1 + a_2 \alpha) \beta + C_{l\delta_p} \delta_p + a_3 a \delta_r \\
 C_m(\alpha, \delta_q) &= C_{m0} + C_{m\alpha} \alpha + C_{m\delta_q} \delta_q \\
 C_n(\delta_r) &= C_{n\delta_r} \delta_r
 \end{aligned} \tag{3.2}$$

For this work the following characteristics were considered:

Mach=2.75, Altitude= 40000ft, $Q=2073,7 \text{ lb ft}^{-2}$, $K_Q = 0.0339s^{-1}$, $I_{xx} = 1.0798$, $I_{yy} = 70.131$,

$$I_{zz} = 70.6609, I_{xz} = -0.7043, I_1 = \frac{I_{xx}I_{xz} + I_{xz}(I_{xx} - I_{yy})}{I_{xx}I_{zz} - I_{xz}^2}, I_2 = \frac{I_{zz}}{I_{xx}I_{zz} - I_{xz}^2},$$

$$I_3 = \frac{I_{xz}}{I_{xx}I_{zz} - I_{xz}^2}, I_4 = \frac{I_{xz}^2 + I_{xx}(I_{xx} - I_{yy})}{I_{xx}I_{zz} - I_{xz}^2}, I_5 = \frac{I_{xx}}{I_{xx}I_{zz} - I_{xz}^2}, \text{Weight}=227 \text{ lb, } S= 0.3068 \text{ ft}^2$$

$$D=7.5 \text{ in, } C_{x0} = -0.4962, C_{x\alpha} = 0.1699, C_{y\beta} = -11.1180, C_{y\delta r} = 4.6346, C_{z\omega} = -0.1006,$$

$$C_{z\alpha} = -27.2417, C_{z\delta q} = -5.4832, a_1 = 1.4008, a_2 = -25.7771, a_3 = -4.4423,$$

$$C_{l\delta p} = -7.2605, C_{m0} = -1.4785, C_{m\alpha} = -5.6355, C_{m\delta q} = -38.7896, C_{n\delta r} = -33.6611.$$

The guidance commands for a BTT airframe may require a large angle of attack and roll rate, while minimizing the sideslip angle. When both the angle of attack and roll rate become large, the dynamic cross coupling nonlinearities become most evident.

As previously noted, the missile dynamics are highly coupled and nonlinear, a high roll rate and angle of attack induce a high yaw rate and pitch/yaw/roll kinematic coupling. [10]

3.2. Model Linearization and Analysis

Before running a Matlab simulation of the previously described control law, and since linear equations are considered one will need to linearize the equation 3.1 at the stabilization point in this case $\alpha = 0^\circ, \beta = 0^\circ, p = q = r = 0, \delta_p = 0^\circ, \delta_q = 0^\circ, \delta_r = 0^\circ$, where

$$x = \begin{pmatrix} \alpha \\ \beta \\ p \\ q \\ r \end{pmatrix} \quad (3.3),$$

$$u = \begin{pmatrix} \delta_p \\ \delta_q \\ \delta_r \end{pmatrix} \quad (3.4)$$

$$\dot{x} = f(x, u) \quad (3.5)$$

the first step will be to linearize the function \dot{x} around the equilibrium point the function obtained is

$$\begin{aligned} \dot{x} &= Ax + Bu \\ y &= Cx \end{aligned} \quad (3.6)$$

given

$$C = \begin{bmatrix} 1 & 0 & 0 & 0 & 0 \\ 0 & 1 & 0 & 0 & 0 \\ 0 & 0 & 1 & 0 & 0 \\ 0 & 0 & 0 & 1 & 0 \\ 0 & 0 & 0 & 0 & 1 \end{bmatrix} \quad (3.7)$$

the matrices A and B are obtained linearizing equation (3.5) A is given by

$$\left. \frac{df}{dx} \right|_{x_{nominal}} \quad (3.8)$$

Or

$$A = \begin{bmatrix} \frac{\partial \dot{\alpha}}{\partial \alpha} & \frac{\partial \dot{\alpha}}{\partial \beta} & \frac{\partial \dot{\alpha}}{\partial p} & \frac{\partial \dot{\alpha}}{\partial q} & \frac{\partial \dot{\alpha}}{\partial r} \\ \frac{\partial \dot{\beta}}{\partial \alpha} & \frac{\partial \dot{\beta}}{\partial \beta} & \frac{\partial \dot{\beta}}{\partial p} & \frac{\partial \dot{\beta}}{\partial q} & \frac{\partial \dot{\beta}}{\partial r} \\ \frac{\partial \dot{p}}{\partial \alpha} & \frac{\partial \dot{p}}{\partial \beta} & \frac{\partial \dot{p}}{\partial p} & \frac{\partial \dot{p}}{\partial q} & \frac{\partial \dot{p}}{\partial r} \\ \frac{\partial \dot{q}}{\partial \alpha} & \frac{\partial \dot{q}}{\partial \beta} & \frac{\partial \dot{q}}{\partial p} & \frac{\partial \dot{q}}{\partial q} & \frac{\partial \dot{q}}{\partial r} \\ \frac{\partial \dot{r}}{\partial \alpha} & \frac{\partial \dot{r}}{\partial \beta} & \frac{\partial \dot{r}}{\partial p} & \frac{\partial \dot{r}}{\partial q} & \frac{\partial \dot{r}}{\partial r} \end{bmatrix} \quad (3.9)$$

The final result is given in the next equation

$$A = \begin{bmatrix} -0.9067 & 0 & 0 & 1 & 0 \\ -0 & -0.3601 & 0 & 0 & -1 \\ 0 & 519.1597 & 0 & 0 & 0 \\ -31.9490 & 0 & 0 & 0 & 0 \\ 0 & -5.1746 & 0 & 0 & 0 \end{bmatrix} \quad (3.10)$$

and B is given by

$$\left. \frac{df}{du} \right|_{u_{nominal}} \quad (3.11)$$

Or

$$B = \begin{bmatrix} \frac{\partial \dot{\alpha}}{\partial \delta_p} & \frac{\partial \dot{\alpha}}{\partial \delta_q} & \frac{\partial \dot{\alpha}}{\partial \delta_r} \\ \frac{\partial \dot{\beta}}{\partial \delta_p} & \frac{\partial \dot{\beta}}{\partial \delta_q} & \frac{\partial \dot{\beta}}{\partial \delta_r} \\ \frac{\partial \dot{p}}{\partial \delta_p} & \frac{\partial \dot{p}}{\partial \delta_q} & \frac{\partial \dot{p}}{\partial \delta_r} \\ \frac{\partial \dot{q}}{\partial \delta_p} & \frac{\partial \dot{q}}{\partial \delta_q} & \frac{\partial \dot{q}}{\partial \delta_r} \\ \frac{\partial \dot{r}}{\partial \delta_p} & \frac{\partial \dot{r}}{\partial \delta_q} & \frac{\partial \dot{r}}{\partial \delta_r} \end{bmatrix} \quad (3.12)$$

The final matrix is given as follow

$$B = \begin{bmatrix} 0 & -0.2 & 0 \\ 0 & 0 & 0.2 \\ -2690.9 & 0 & 124.3 \\ 0 & -219.9 & 0 \\ 26.8 & 0 & -192.3 \end{bmatrix} \quad (3.13)$$

The controllability can be analyzed with the command `ctrb` in Matlab and the result was that the system is controllable this command computes the controllability matrix for the matrices A and B in the form of

$$\Delta = [B \ AB \ A^2B \ A^3B \ A^{n-1}B] \quad (3.14),$$

the controllability denotes the ability to move a system around in its entire configuration space, this mean that we can take an initial state and replace it by a final with no change in the system, it also implies that for every value of A, a value of B will exist. The system is controllable only if Δ has n independent columns ($\text{rank}(\Delta)=n$) the Kalman duality theorem that explains controllability will be explained later

The observability can be analyzed with the control `obsv` no Matlab and the result was n observable this command computes the observability matrix for state-space system using A and C matrices as follow

$$\Gamma = \begin{bmatrix} C \\ CA \\ CA^2 \\ CA^3 \\ CA^{n-1} \end{bmatrix} \quad (3.15)$$

the observability states that for every output in the state space, the input can be determined the system will only be observable if ($\text{rank}(\Gamma)=n$) in the same way as controllability the Kalman duality theorem that also explains observability will be explained next

The Kalman duality theorem states that a system in the form

$$\left(\Sigma^*\right) \begin{cases} \dot{z} = A^*z + C^*v \\ w = B^*z + D^*v \end{cases} \quad (3.16)$$

Where z is the state function w the observability function and v the controllability function, knowing this it is possible to state that

$$\begin{aligned} (1) \quad & (\Sigma) \text{controllable} \Rightarrow (\Sigma^*) \text{observable} \\ (2) \quad & (\Sigma) \text{observable} \Rightarrow (\Sigma^*) \text{controllable} \end{aligned} \quad (3.17)$$

The last equation states that if a system is controllable then its dual state is observable and in the same way if a system is observable its dual system will be observable.

3.3. Minimum Variance Controller Design

Since the minimum variance controller is discrete, the matrices A and B will be discretize the result are given as follow

$$A_d = \begin{bmatrix} 0.9894 & 0 & 0 & 0.0100 & 0 \\ 0 & 0.9967 & 0 & 0 & -0.0100 \\ 0 & 5.1822 & 1 & 0 & -0.0260 \\ -0.3180 & 0 & 0 & 0.9984 & 0 \\ 0 & -0.0517 & 0 & 0 & 1.0003 \end{bmatrix} \quad (3.18)$$

And

$$B_d = \begin{bmatrix} 0 & -0.0128 & 0 \\ -0.0013 & 0 & 0.0112 \\ -26.9109 & 0 & 1.2642 \\ 0 & -2.1976 & 0 \\ 0.2682 & 0 & -1.9236 \end{bmatrix} \quad (3.19)$$

The equations used for the discretization are given as follow

$$A_h = A * dt \quad (3.20)$$

$$A_d = I + A_h + \frac{1}{2} A_h^2 \quad (3.21)$$

$$B_d = \left(I + \frac{1}{2} A_h + \frac{1}{6} A_h^2 \right) dt * B \quad (3.22)$$

where A_h represents the step of the discretization of the matrix A, dt represents the time step used, I represent an identity matrix.

Using the equations of a discrete LQR controller it is possible to obtain the matrix P using the matrices Ad, Bd and two other matrices identity one of rank 5 and the other of rank 3.

$$P = \begin{bmatrix} 46.5710 & 0 & 0 & 0.2037 & 0 \\ 0 & 72.8544 & 0.0057 & 0 & 0.4560 \\ 0 & 0.0057 & 1.0014 & 0 & 0.0030 \\ 0.2037 & 0 & 0 & 1.1770 & 0 \\ 0 & -0.4560 & 0.0030 & 0 & 1.2271 \end{bmatrix} \quad (3.23)$$

Example 1- Analysis at flight conditions $\alpha = 10^\circ$, $\beta = 2^\circ$, $p = q = r = 0$, $\delta_p = 10^\circ$, $\delta_q = 20^\circ$, $\delta_r = 8^\circ$ for the reference conditions $\alpha^* = 0$, $\beta^* = 0$, $p^* = q^* = r^* = 0$

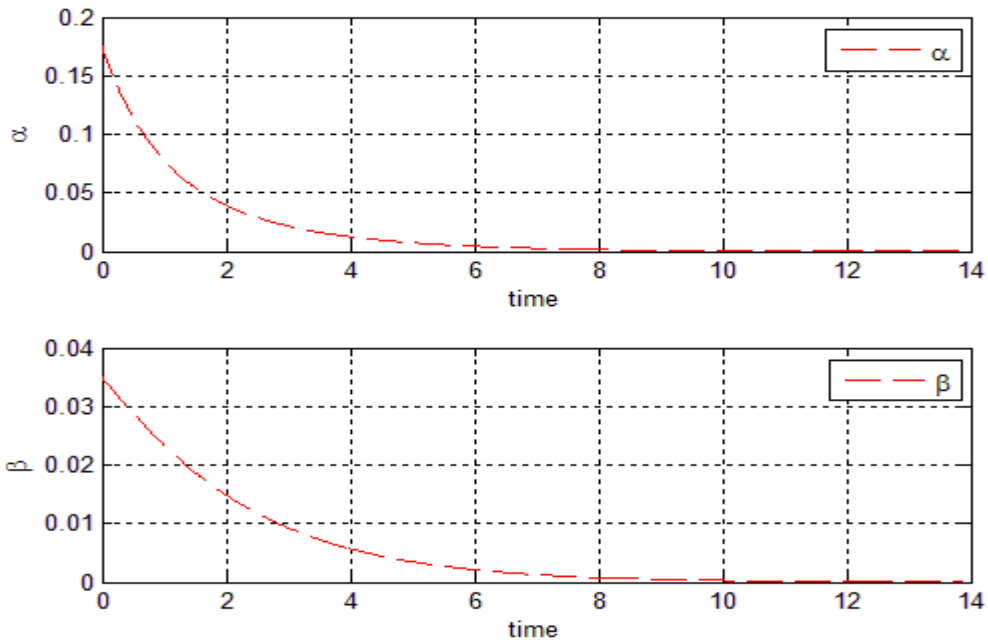


Figure 3.1- Variation of angle of attack α and sideslip angle β with time for the conditions $\alpha = 10^\circ$, $\beta = 2^\circ$, $p = q = r = 0$, $\delta_p = 10^\circ$, $\delta_q = 20^\circ$

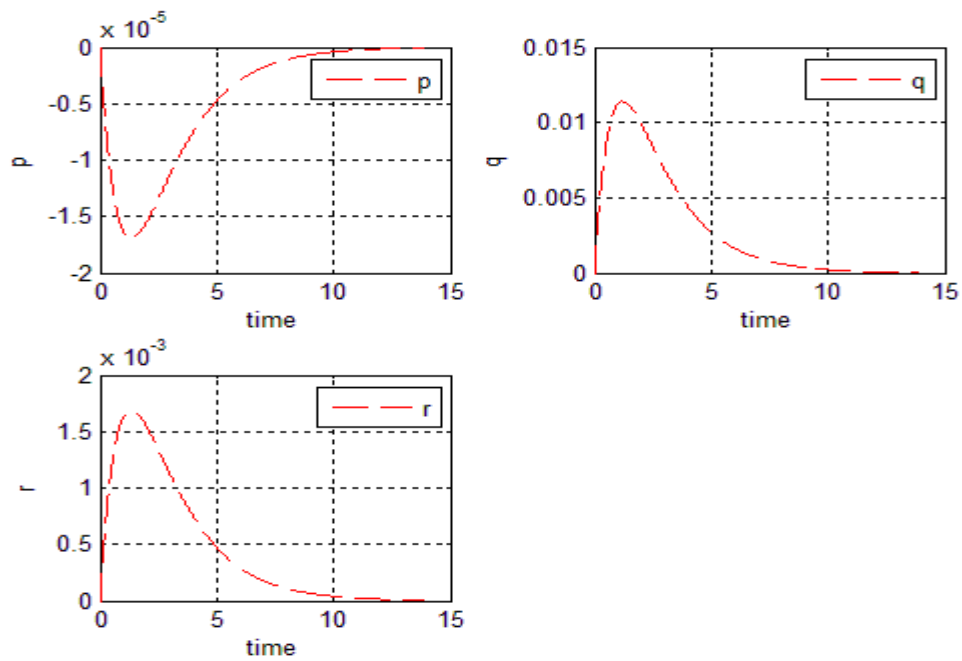


Figure 3.2- Variation of the roll p , the pitch q and the yaw r with time for the conditions $\alpha = 10^\circ$, $\beta = 2^\circ$, $p = q = r = 0$, $\delta_p = 10^\circ$, $\delta_q = 20^\circ$

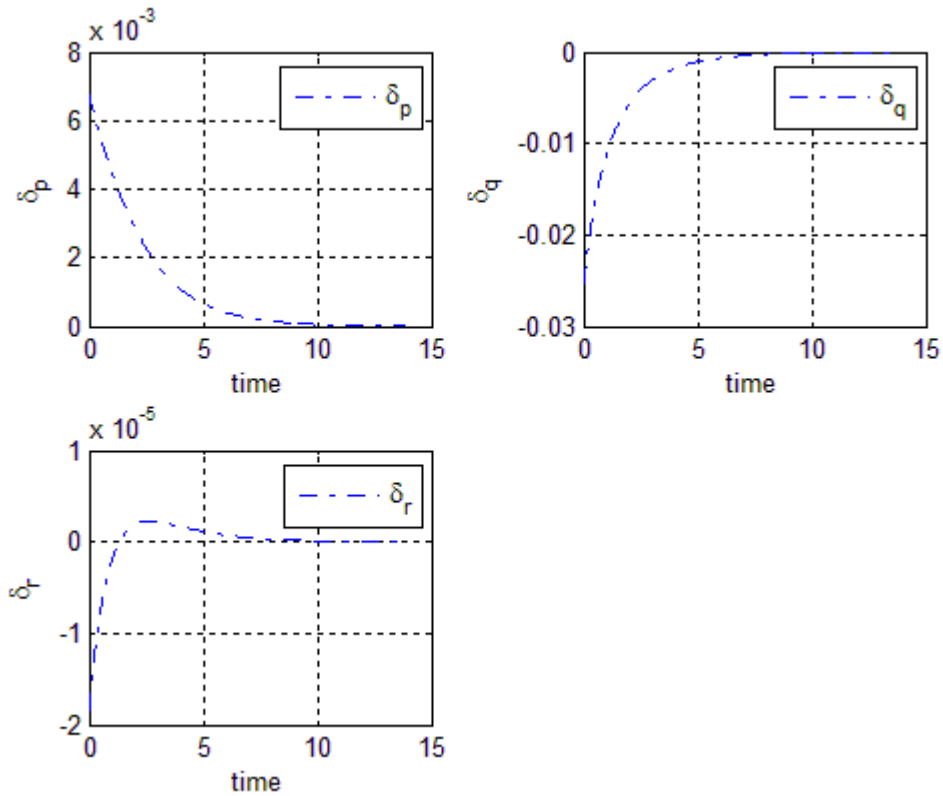


Figure 3.3- Variation of the roll controller δ_p , the pitch controller δ_q and the yaw controller δ_r with time for the conditions $\alpha = 10^\circ$, $\beta = 2^\circ$, $p = q = r = 0$, $\delta_p = 10^\circ$, $\delta_q = 20^\circ$

In Figs. 3.1 to 3.3 it is possible to see the stabilization of the various parameters tested.

Fig. 3.1 shows the variation of the angle of attack and as one can see it decreases continuously until stabilization at zero in about 8 seconds, one can also see in the same figure, the stabilization of the sideslip angle and as it is possible to see it continuously decreases until it reaches zero in nearly 10 seconds.

Fig. 3.2 shows the roll variation where one can see it decreases until it reaches the minimum of -1.67 radian per seconds in 1.6 seconds and then rises until it reaches zero after almost 14 seconds, it is also possible to see the variation of the pitch angle that increases up to 0.011 radian per seconds in 1.6 second and then decreases to zero in nearly 14 seconds, it stills represents the variation of yaw that rises to 0.0017 radian per seconds in 1.6 seconds and then descends to zero in around 14 seconds.

In fig. 3.3 one can see the variation of the roll controller that decreases continuously in 14 seconds until it reaches zero, it is also possible to see the variation of the pitch controller that rises up to zero in 9 seconds, it stills represents the variation of the yaw controller that rises to zero in 1.8 seconds then rise to 0.000025 radian per seconds at the 2.2 seconds and then stabilize at zero in 8 seconds.

Example 2- Analysis at flight conditions $\alpha = 1^\circ$, $\beta = 0.2^\circ$, $p = q = r = -50$, $\delta_p = 10^\circ$, $\delta_q = 20^\circ$, $\delta_r = 8^\circ$ for the reference conditions $\alpha^* = 0$, $\beta^* = 0$, $p^* = q^* = r^* = 0$

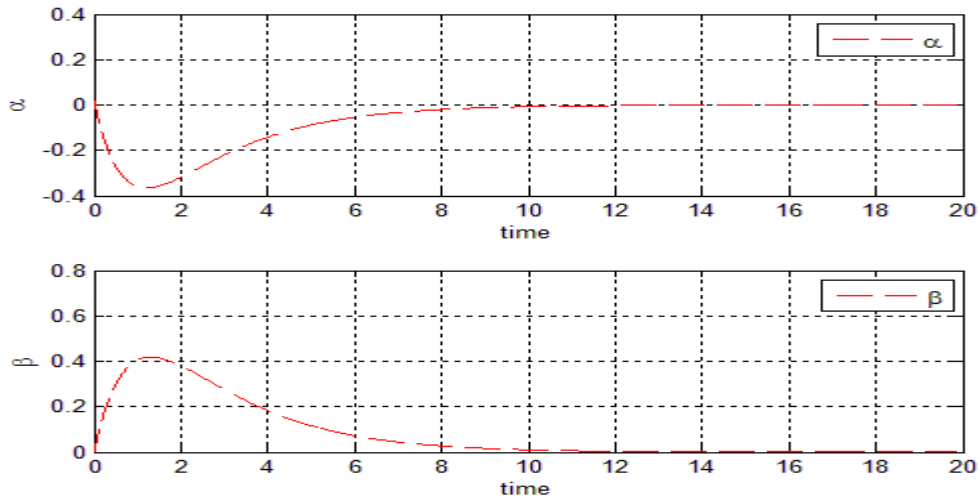


Figure 3.4- Variation of angle of attack α and the sideslip angle with time for the conditions $\alpha = 1^\circ$, $\beta = 0.2^\circ$, $p = q = r = -50$, $\delta_p = 10^\circ$, $\delta_q = 20^\circ$, $\delta_r = 8^\circ$

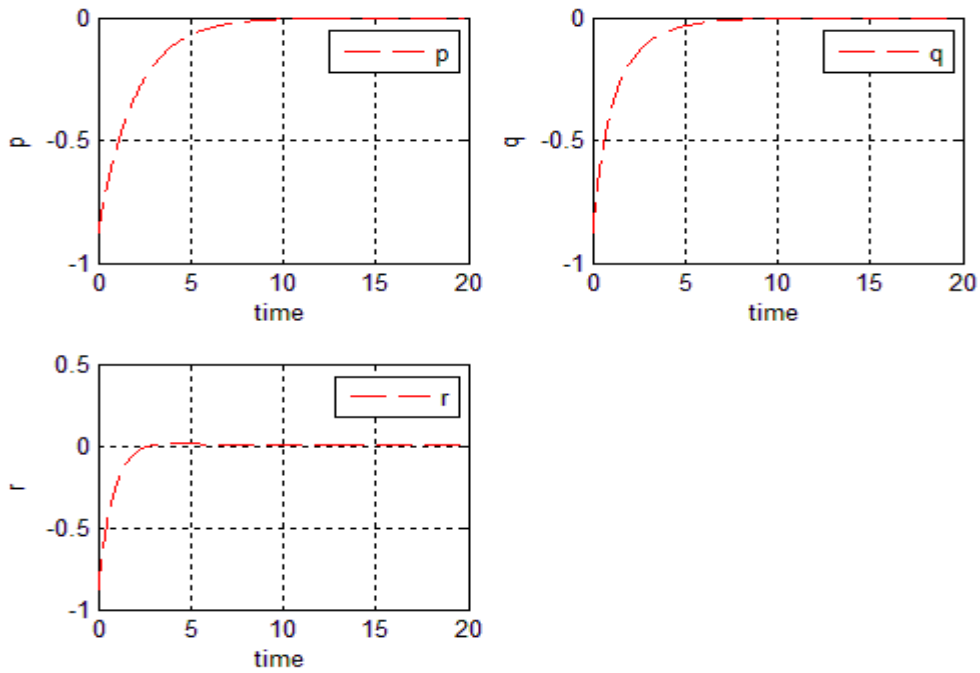


Figure 3.5- Variation of roll p , pitch q and yaw r with time for the conditions $\alpha = 1^\circ$, $\beta = 0.2^\circ$, $p = q = r = -50$, $\delta_p = 10^\circ$, $\delta_q = 20^\circ$, $\delta_r = 8^\circ$

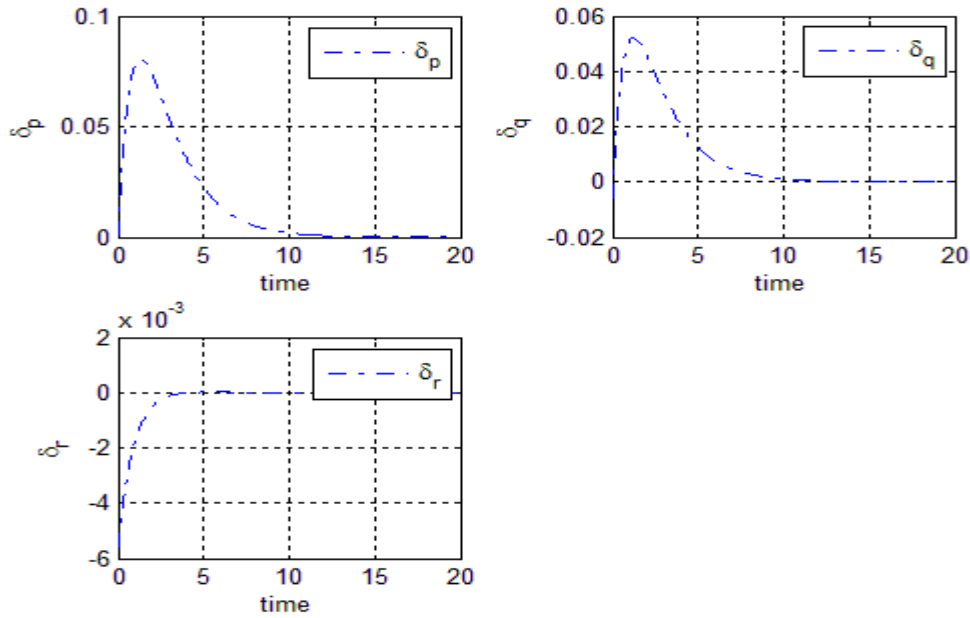


Figure 3.6- Variation of roll controller angle δ_p , pitch controller angle δ_q and yaw controller angle δ_r with time for the conditions $\alpha = 1^\circ$, $\beta = 0.2^\circ$, $p = q = r = -50$, $\delta_p = 10^\circ$, $\delta_q = 20^\circ$, $\delta_r = 8^\circ$

In Figs 3.4 to 3.6 it is possible to see the stabilization of the various parameters tested.

In fig. 3.4 it is possible to see the variation of the angle of attack and as it is possible to see it decreases down to -0.37 radian per second in around 1 second and then rise until stabilization at zero in about 12 seconds, one can also see the stabilization of the sideslip angle and as it is possible to see it increases until it reaches 0.42 radian per second in nearly 1 second then decreases to zero in nearly 14 seconds.

Fig. 3.5 shows the roll variation that continuously increases until it reaches zero in 12 seconds, it is also possible to see the variation of the pitch continuously increases until it reaches zero in 10 seconds, this figure also represents the variation of yaw that rises to 0.00017 radian per seconds in 3 seconds and then descends to zero in around 12 seconds.

In fig. 3.6 one can see the variation of the roll controller that increases up to 0.08 in 1 second and then descends to zero in 14 seconds, it is also possible to see the variation of the pitch controller that rises up to 0.051 radian per seconds in 1 second and then decreases to zero in 13 seconds, it also represents the variation of the yaw controller that rises continuously to zero in 3 seconds.

The next set of figures are obtained using the reference point $\alpha^* = 20^\circ$, $\beta^* = p^* = q^* = r^* = 0$.

For these reference point the matrix A is as follow

$$A = \begin{bmatrix} -0.7 & 0 & 0 & 1 & 0 \\ 0 & -0.3 & -0.3 & 0 & -0.9 \\ 0 & -2815.6 & 0 & 0 & 0 \\ -31.9 & 0 & 0 & 0 & 0 \\ 0 & 28.1 & 0 & 0 & 0 \end{bmatrix} \quad (3.24)$$

The matrix B is given as follow

$$B = \begin{bmatrix} 0 & -0.2 & 0 \\ 0 & 0 & 0.2 \\ -2690.9 & 0 & 124.3 \\ 0 & -219.9 & 0 \\ 26.8 & 0 & -192.3 \end{bmatrix} \quad (3.25)$$

The matrix Ad is given as follow

$$A_d = \begin{bmatrix} 0.9910 & 0 & 0 & 0.0100 & 0 \\ 0 & 1.0443 & -0.0034 & 0 & -0.0094 \\ 0 & -28.1207 & 1.0481 & 0 & -0.1323 \\ -0.3180 & 0 & 0 & 0.9984 & 0 \\ 0 & 0.2803 & -0.0005 & 0 & 0.9987 \end{bmatrix} \quad (3.26)$$

The matrix Bd is given as follow

$$B_d = \begin{bmatrix} 0 & -0.0127 & 0 \\ -0.0447 & 0 & 0.0180 \\ -27.3287 & 0 & -4.6802 \\ 0 & -2.1976 & 0 \\ 0.2724 & 0 & -1.8644 \end{bmatrix} \quad (3.27)$$

The Matrix P is given as follow

$$P = \begin{bmatrix} 52.7101 & 0 & 0 & 0.2425 & 0 \\ 0 & 131.669 & -0.2524 & 0 & -0.6690 \\ 0 & -0.2524 & 1.0018 & 0 & 0.0009 \\ 0.2425 & 0 & -0 & 1.1772 & 0 \\ 0 & -0.6690 & 0.0009 & 0 & 1.2328 \end{bmatrix} \quad (3.28)$$

Example 3- Analysis at flight conditions $\alpha = 10^\circ$, $\beta = 2^\circ$, $p = q = r = 0$, $\delta_p = 10^\circ$, $\delta_q = 20^\circ$, $\delta_r = 8^\circ$ for the reference condition $\alpha^* = 20^\circ$, $\beta^* = p^* = q^* = r^* = 0$

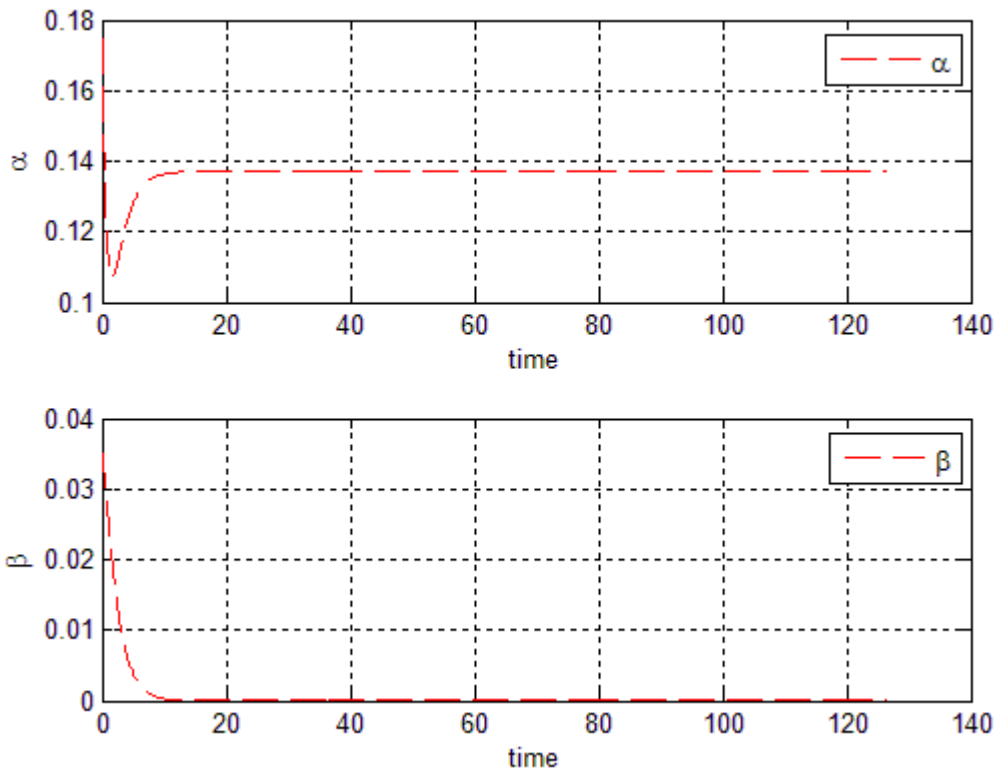


Figure 3.7- Variation of angle of attack α and the sideslip angle β with time for the conditions $\alpha = 10^\circ$, $\beta = 2^\circ$, $p = q = r = 0$, $\delta_p = 10^\circ$, $\delta_q = 20^\circ$

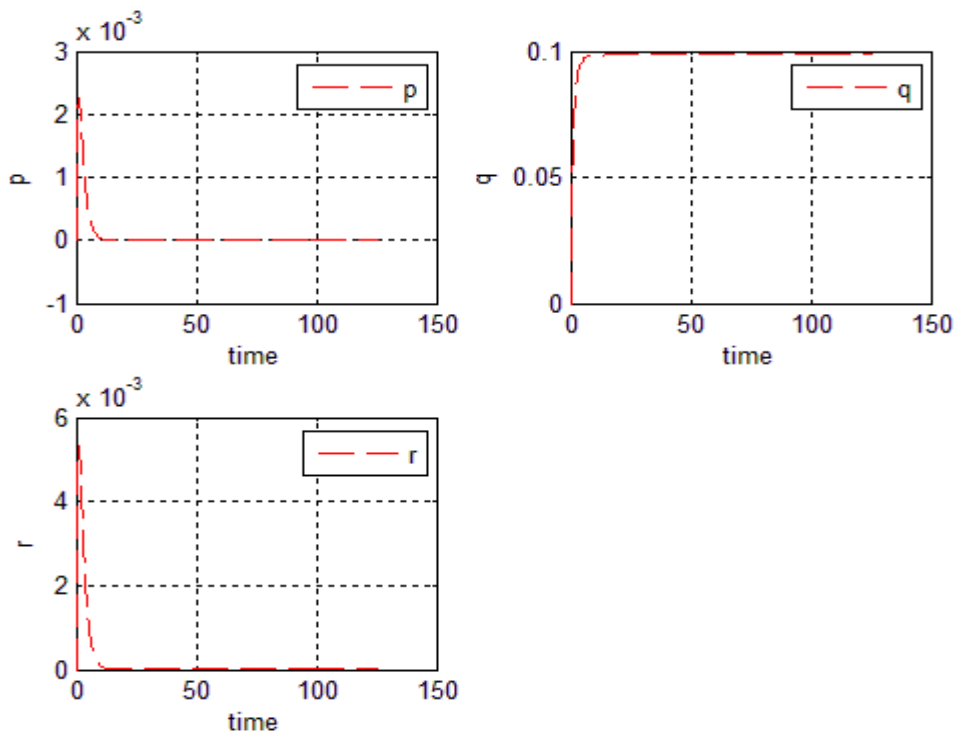


Figure 3.8- Variation of the roll p , the pitch q and the yaw r with time for the conditions $\alpha = 10^\circ$, $\beta = 2^\circ$, $p = q = r = 0$, $\delta_p = 10^\circ$, $\delta_q = 20^\circ$

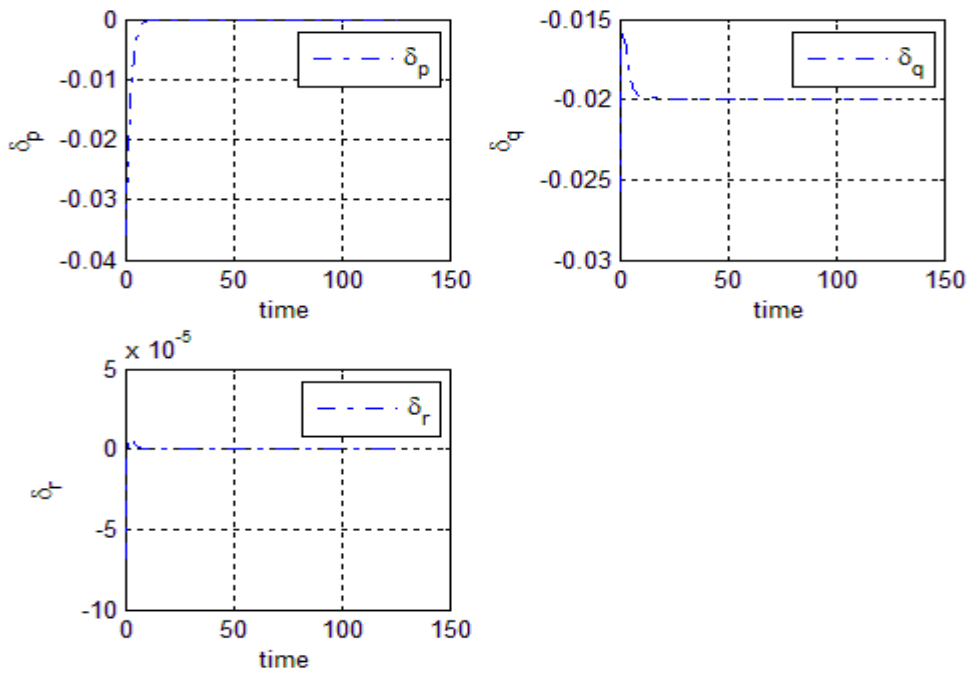


Figure 3.9- Variation of the roll controller angle δ_p , the pitch controller angle δ_q and the yaw controller angle δ_r with time for the conditions $\alpha=10^\circ, \beta=2^\circ, p=q=r=0, \delta_p=10^\circ, \delta_q=20^\circ$

In Figs 3.7 to 3.9 it is possible to see the stabilization of the various parameters tested.

In fig. 3.7 it is possible to see the variation of the angle of attack and as one can see it decreases up to 0.11 radian per second in around 1 second and then increases until stabilization at 0.137 radian per second in about 12 seconds, one can also see the stabilization of the sideslip angle and as it is possible to see it decreases continuously down to zero in nearly 12 seconds.

Fig. 3.8 shows the roll variation that increases up to 0.215 radian per second in around 1 second and then decreases to zero in 12 seconds, it is also possible to see the variation of the pitch increases continuously up to nearly 0.1 radian per second, it also represents the variation of yaw that increases up to 0.051 radian per seconds in 1 second and reaches zero in 14 seconds.

In fig. 3.9 one can see the variation of the roll controller that increases continuously up to zero in around 12 seconds, it is also possible to see the variation of the pitch controller that increases up to -0.016 radian per seconds in 1 second and then descends to -0.02 in 12 seconds, it also represents the variation of the yaw controller that increases to 0.00001 radian per second in 1 second and then descends to zero in 10 seconds.

After running the previous analyses it is possible to see that for the first reference point chosen the system is stable there for confirming that the system is stable in the origin.

It is also possible to see that the system is robust since it as a very large area of stabilization and one can also observe that it takes a relatively short amount of time to the system to stabilize itself, for the other reference point chosen it is possible to see that those points are stable in the latero-directional part of the flight due to the fact that the sideslip angle the roll, the yaw and the roll and yaw respective controller tend in all tested points to zero while in the longitudinal part of the flight is stable in one point since the angle of attack, the pitch

and the pitch controller tends to zero but is unstable for all the others tested points since the angle of attack, the pitch and the pitch controller don't tend to zero.

One can also see that once the flight condition reaches the stabilizing conditions he stays in a very small interval around the stabilizing conditions.

3.4. H-infinity Controller Design

The first step of this simulation as the minimum variance one, the H-infinity simulation is linear the state equations will be linearized and the results are given as follow

$$A = \begin{bmatrix} -0.9067 & 0 & 0 & 1 & 0 \\ -0 & -0.3601 & 0 & 0 & -1 \\ 0 & 519.1597 & 0 & 0 & 0 \\ -31.9490 & 0 & 0 & 0 & 0 \\ 0 & -5.1746 & 0 & 0 & 0 \end{bmatrix} \quad (3.29)$$

And

$$B = \begin{bmatrix} 0 & -0.2 & 0 \\ 0 & 0 & 0.2 \\ -2690.9 & 0 & 124.3 \\ 0 & -219.9 & 0 \\ 26.8 & 0 & -192.3 \end{bmatrix} \quad (3.30)$$

After the linearization we need to obtain the gain, using reference [7] the first step will be to solve the following equation to obtain the gain,

$$PA + PA^T + Q + \frac{1}{\gamma^2} PDD^T P - PBR^{-1}B^T P + LR^{-1}L = 0 \quad (3.31)$$

Since C is an identity matrix then L will be 0, $Q = C^T C$ and since disturbance was used D is given as follow

$$D = \begin{bmatrix} 0 & 0 \\ 0 & 0.1 \\ 0.1 & 0 \\ 0 & 0 \\ 0 & 0 \end{bmatrix} \quad (3.32)$$

Since P will be obtained using a Riccati equation the following equations will be used

$$PA + PA^T + P(\gamma^{-2}DD^T - BB^T)P + Q = 0 \quad (3.33)$$

After rewriting the last equation in the Riccati equation form one obtain the following equation

$$PA + PA^T + P\bar{B}R\bar{B}^T P + Q = 0 \quad (3.34)$$

Where \bar{B} is given by $[D, B]$,

$$R = \begin{bmatrix} -0.0441 & 0 & 0 & 0 & 0 \\ 0 & -0.0441 & 0 & 0 & 0 \\ 0 & 0 & 1 & 0 & 0 \\ 0 & 0 & 0 & 1 & 0 \\ 0 & 0 & 0 & 0 & 1 \end{bmatrix} \quad (3.35)$$

After solving the Riccati equation the matrix P is obtain and given as follow

$$P = \begin{bmatrix} 0.5220 & 0 & 0 & 0.0013 & 0 \\ 0 & 1.3587 & -0.0005 & 0 & -0.0047 \\ 0 & -0.0005 & 0.0004 & 0 & 0 \\ 0.0013 & 0 & 0 & 0.0046 & 0 \\ 0 & -0.0047 & 0 & 0 & 0.0053 \end{bmatrix} \quad (3.36)$$

The gain will be given by the following equation

$$K = R^{-1}(B^T P + L) \quad (3.37)$$

And in this conditions the gain is

$$K = \begin{bmatrix} 0 & -0.0017 & -0.01 & 0 & -0.0003 \\ -0.0031 & 0 & 0 & -0.0100 & 0 \\ 0 & 0.0078 & 0.0003 & 0 & -0.01 \end{bmatrix} \quad (3.38)$$

Knowing the gain it is possible to simulate for any given condition

Example 5- Analysis at flight conditions $\alpha = 10^\circ$, $\beta = 2^\circ$, $p = q = r = 0$, $\delta_p = 10^\circ$, $\delta_q = 20^\circ$, $\delta_r = 8^\circ$ for the reference conditions $\alpha^* = 0$, $\beta^* = 0$, $p^* = q^* = r^* = 0$

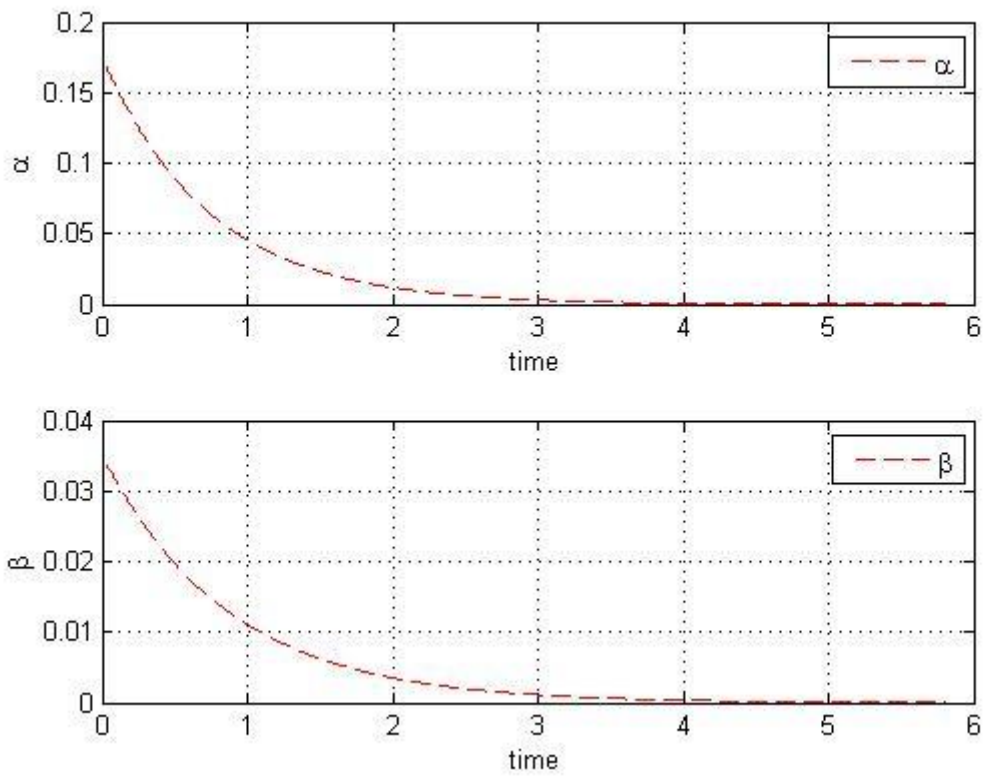


Figure 3.10- Variation of angle of attack α and sideslip angle β with time for the conditions $\alpha = 10^\circ$, $\beta = 2^\circ$, $p = q = r = 0$, $\delta_p = 10^\circ$, $\delta_q = 20^\circ$

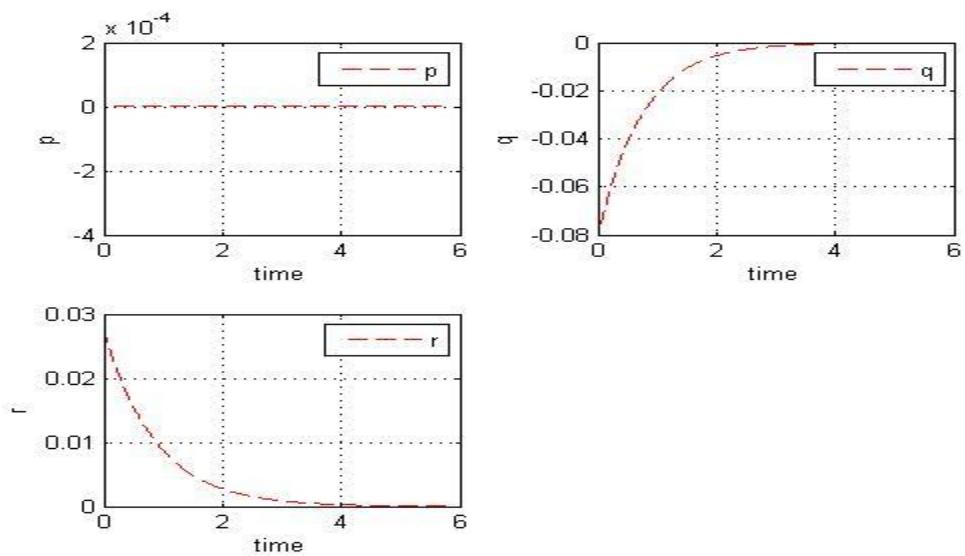


Figure 3.11- Variation of the roll p , the pitch q and the yaw r with time for the conditions $\alpha = 10^\circ$, $\beta = 2^\circ$, $p = q = r = 0$, $\delta_p = 10^\circ$, $\delta_q = 20^\circ$

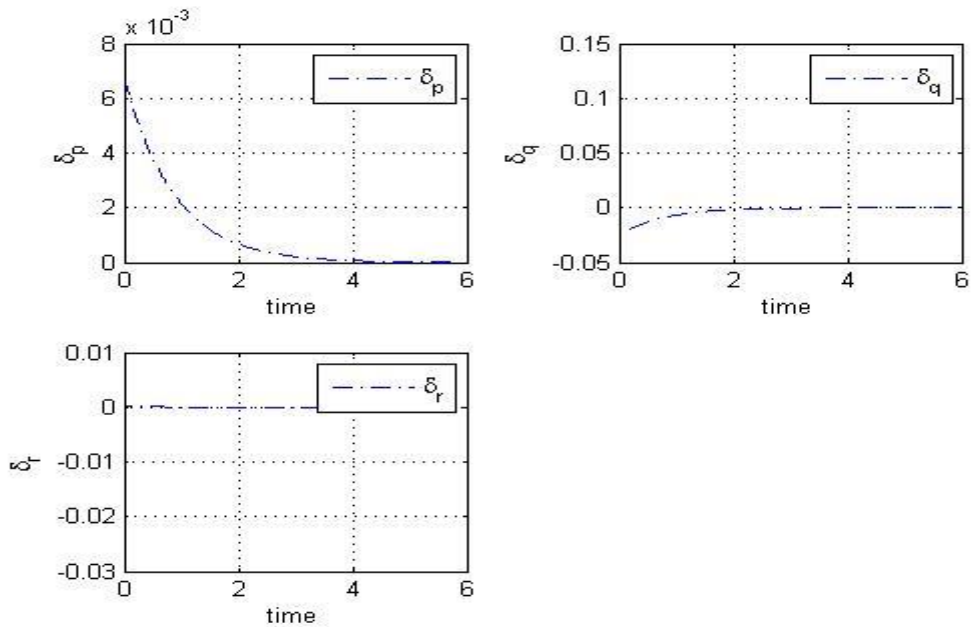


Figure 3.12- Variation of the roll controller δ_p , the pitch controller δ_q and the yaw controller δ_r with time for the conditions $\alpha = 10^\circ$, $\beta = 2^\circ$, $p = q = r = 0$, $\delta_p = 10^\circ$, $\delta_q = 20^\circ$

In Figs. 3.10 to 3.12 it is possible to see the stabilization of the various parameters tested.

Fig. 3.10 shows the variation of the angle of attack and as one can see it decreases continuously until stabilization at zero in about 4 seconds, one can also see in the same figure, the stabilization of the sideslip angle and as it is possible to see it continuously decreases until it reaches zero in nearly 4 seconds.

In fig. 3.11 it is shown the roll variation where we can see that it stays at zero, it is also possible to see the variation of the pitch angle that increases continuously up to zero in 4 seconds, it stills represents the variation of yaw that descends continuously to zero in around 4 seconds.

In fig. 3.12 one can see the variation of the roll controller that decreases continuously down to zero in around 4 seconds until it reaches zero, it is also possible to see the variation of the pitch controller that rises up to zero in around 4 seconds, it stills represents the variation of the yaw controller that descends to zero in about 1 seconds.

Example 6- Analysis at flight conditions $\alpha = 1^\circ$, $\beta = 0.2^\circ$, $p = q = r = -50$, $\delta_p = 10^\circ$, $\delta_q = 20^\circ$, $\delta_r = 8^\circ$ for the reference conditions $\alpha^* = 0$, $\beta^* = 0$, $p^* = q^* = r^* = 0$

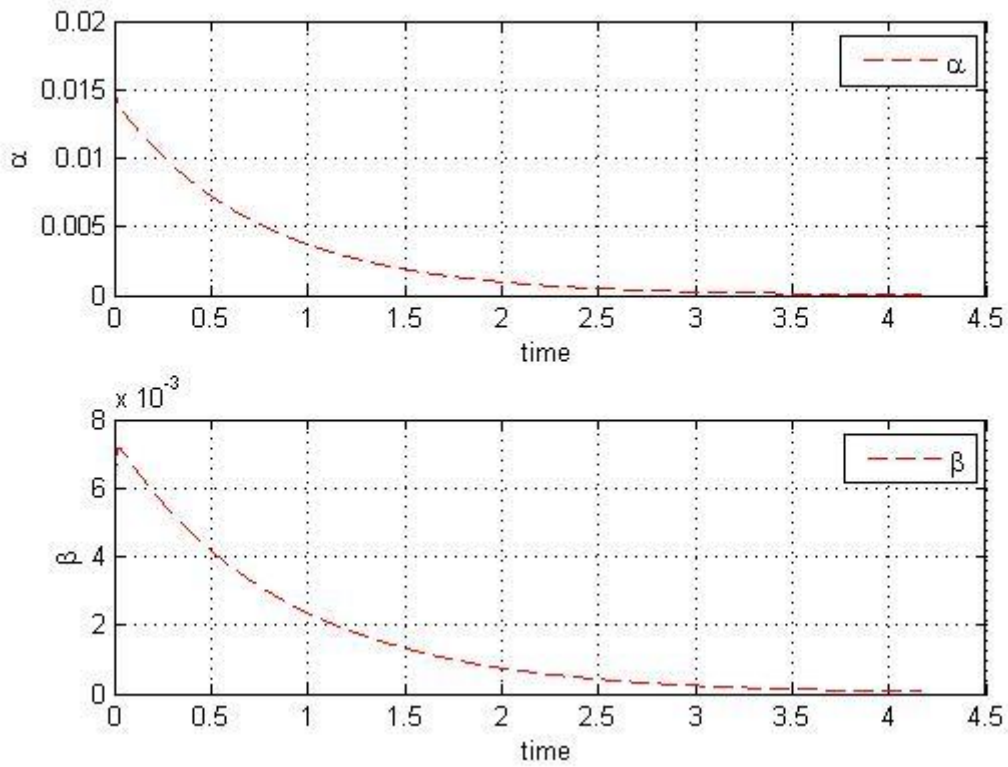


Figure 3.13- Variation of angle of attack α and the sideslip angle with time for the conditions $\alpha = 1^\circ$, $\beta = 0.2^\circ$, $p = q = r = -50$, $\delta_p = 10^\circ$, $\delta_q = 20^\circ$, $\delta_r = 8^\circ$

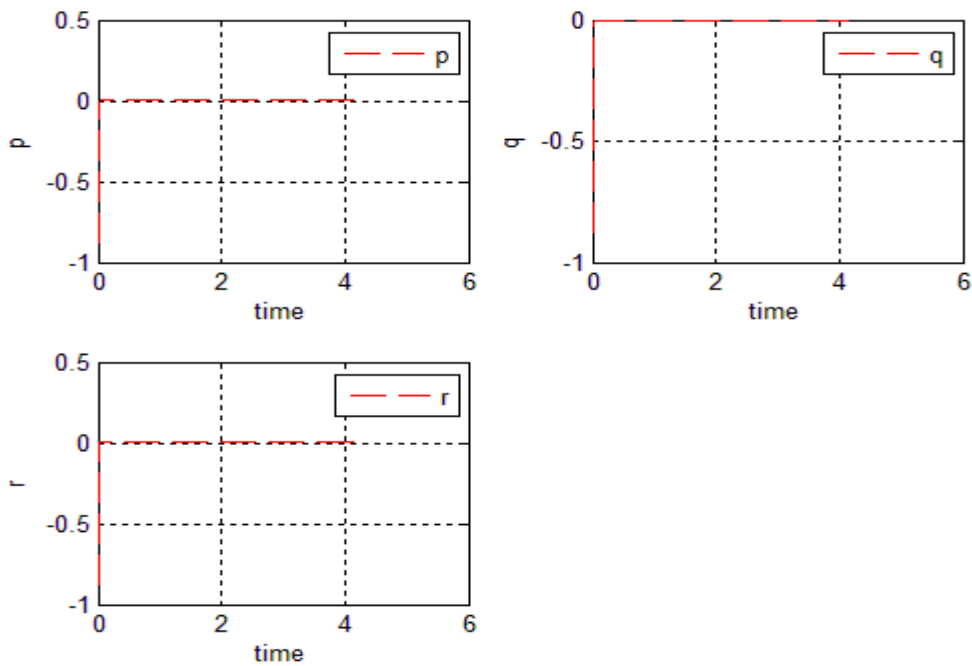


Figure 3.14- Variation of roll p , pitch q and yaw r with time for the conditions $\alpha = 1^\circ$, $\beta = 0.2^\circ$, $p = q = r = -50$, $\delta_p = 10^\circ$, $\delta_q = 20^\circ$, $\delta_r = 8^\circ$

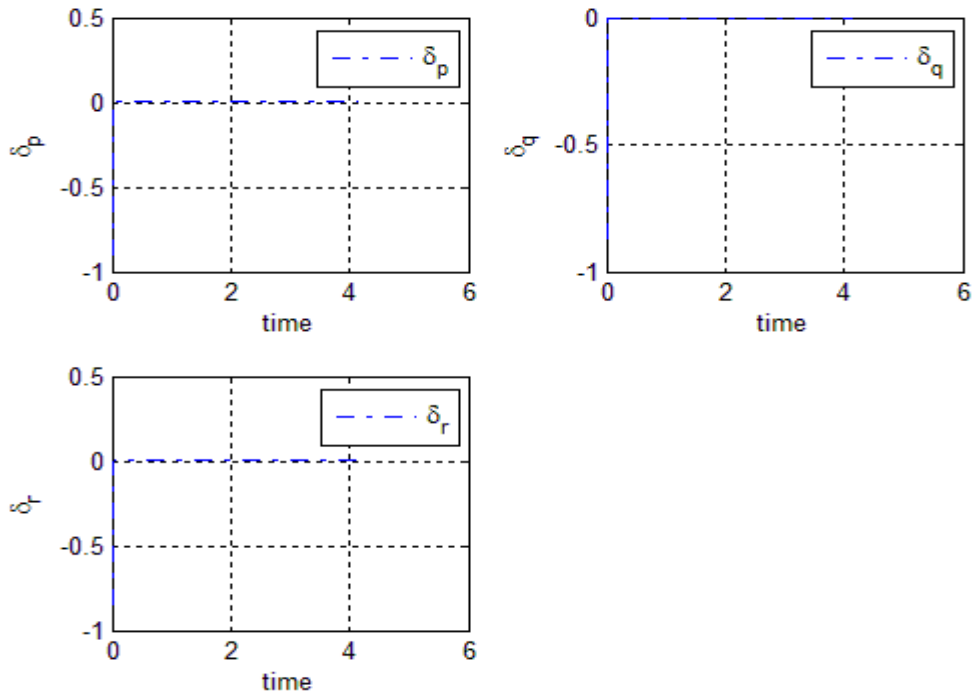


Figure 3.15- Variation of roll controller angle δ_p , pitch controller angle δ_q and yaw controller angle δ_r with time for the conditions $\alpha = 1^\circ$, $\beta = 0.2^\circ$, $p = q = r = -50$, $\delta_p = 10^\circ$, $\delta_q = 20^\circ$, $\delta_r = 8^\circ$

In Figs 3.13 to 3.15 it is possible to see the stabilization of the various parameters tested.

In fig. 3.13 it is possible to see the variation of the angle of attack and as one can see it decreases down to zero in around 4 second, one can also see the stabilization of the sideslip angle and as it is possible to see it decreases continuously down to zero in nearly 4 seconds.

Fig. 3.14 shows that all the figures stay at zero during this experiment.

In fig. 3.15 shows that all the figures stay at zero during this experiment.

Example 7- Analysis at flight conditions $\alpha = 10^\circ$, $\beta = 2^\circ$, $p = q = r = 0$, $\delta_p = 10^\circ$, $\delta_q = 20^\circ$, $\delta_r = 8^\circ$ for the reference condition $\alpha^* = 20^\circ$, $\beta^* = p^* = q^* = r^* = 0$

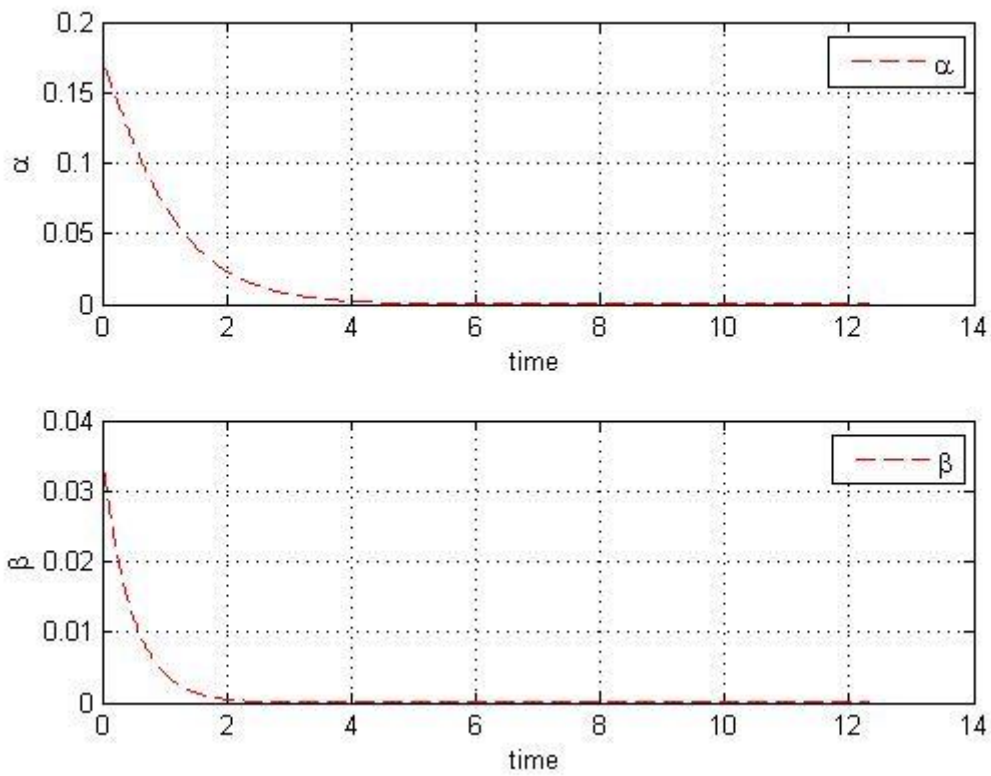


Figure 3.16- Variation of angle of attack α and the sideslip angle β with time for the conditions $\alpha = 10^\circ$, $\beta = 2^\circ$, $p = q = r = 0$, $\delta_p = 10^\circ$, $\delta_q = 20^\circ$

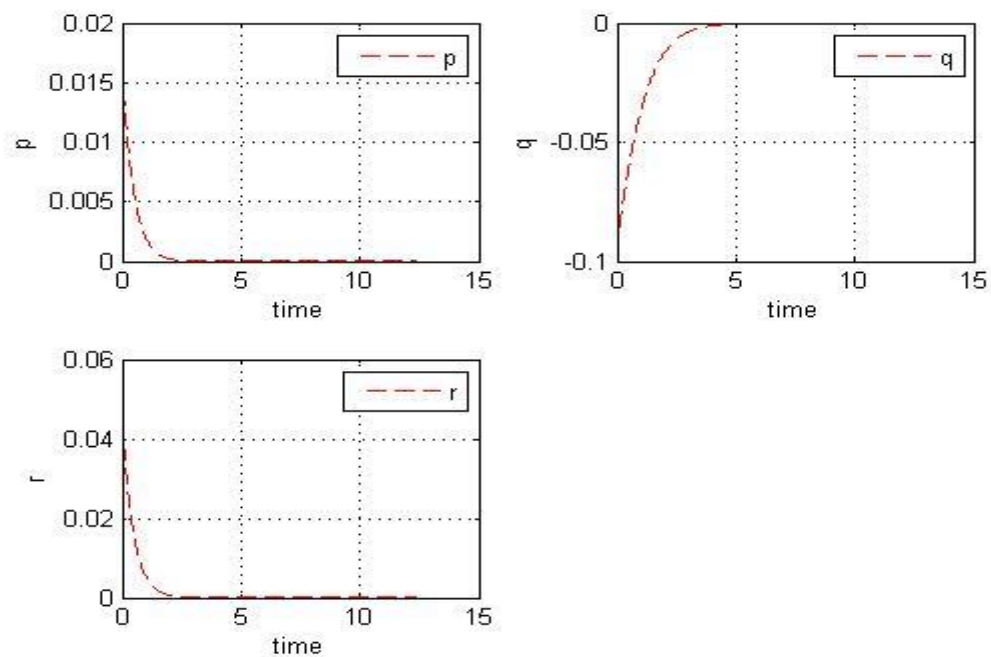


Figure 3.17- Variation of the roll p , the pitch q and the yaw r with time for the conditions $\alpha = 10^\circ$, $\beta = 2^\circ$, $p = q = r = 0$, $\delta_p = 10^\circ$, $\delta_q = 20^\circ$

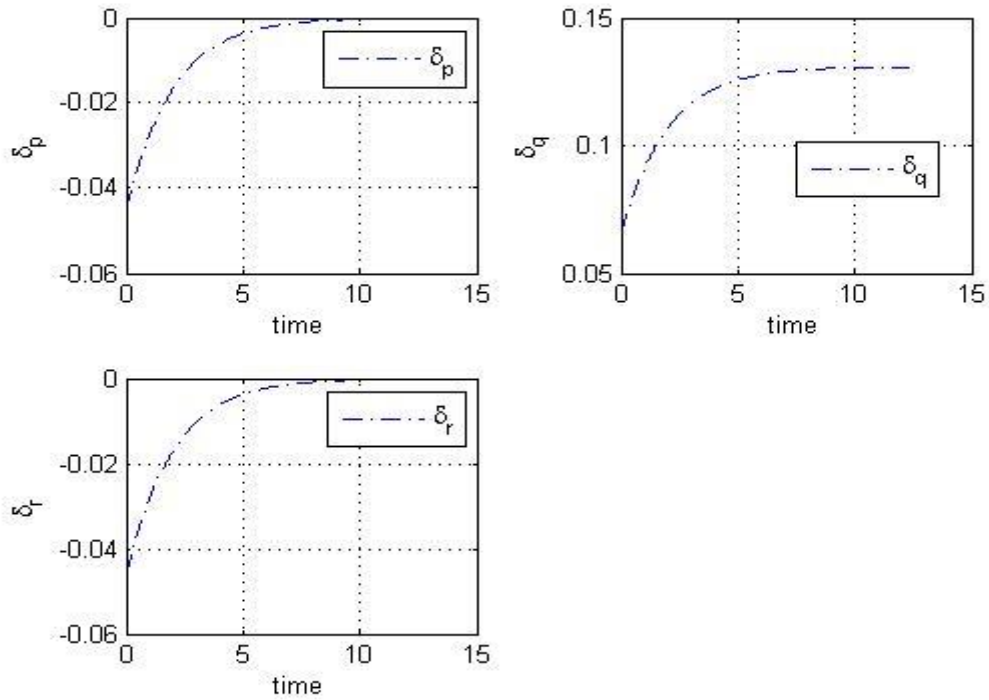


Figure 3.18- Variation of the roll controller angle δ_p , the pitch controller angle δ_q and the yaw controller angle δ_r with time for the conditions $\alpha = 10^\circ$, $\beta = 2^\circ$, $p = q = r = 0$, $\delta_p = 10^\circ$, $\delta_q = 20^\circ$

In Figs 3.16 to 3.18 it is possible to see the stabilization of the various parameters tested.

In fig. 3.16 it is possible to see the variation of the angle of attack and as one can see it decreases down to zero in around 4 seconds, one can also see the stabilization of the sideslip angle and as it is possible to see it decreases continuously down to zero in nearly 3 seconds.

Fig. 3.17 shows the roll variation that decreases down to zero in around 4 seconds, it is also possible to see the variation of the pitch increases up to zero in 5 seconds, it also represents the variation of yaw that decreases down to zero in 5 seconds.

In fig. 3.18 one can see the variation of the roll controller that increases continuously up to zero in around 10 seconds, it is also possible to see the variation of the pitch controller that increases up to 0.125 radian per seconds in 10 seconds, it also represents the variation of the yaw controller that increases up to zero in 10 seconds.

3.5. Comparison

After simulating the two methods, one can compare them for a better understanding of the differences between them and the graphics that shows the difference will now be presented.

The following set of figures shows the superposition between both methods for examples 1 and 5

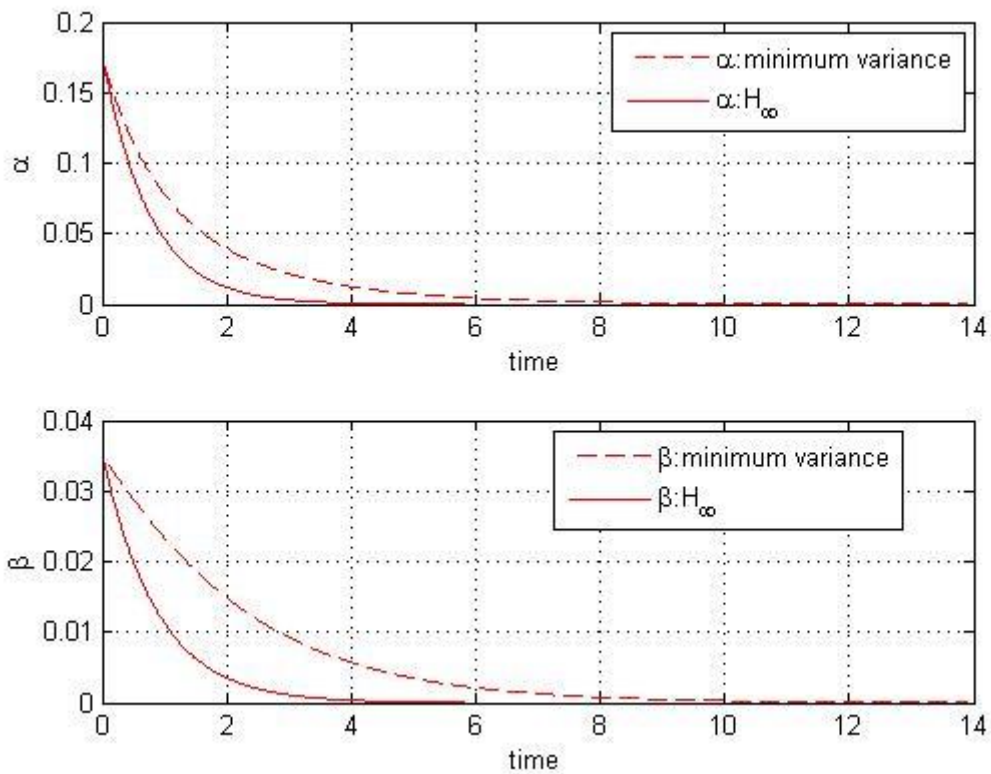


Figure 3.19 Comparison between the minimum variance and H infinity methods for the angle of attack α and the sideslip angle β for the conditions given at examples 1 and 5

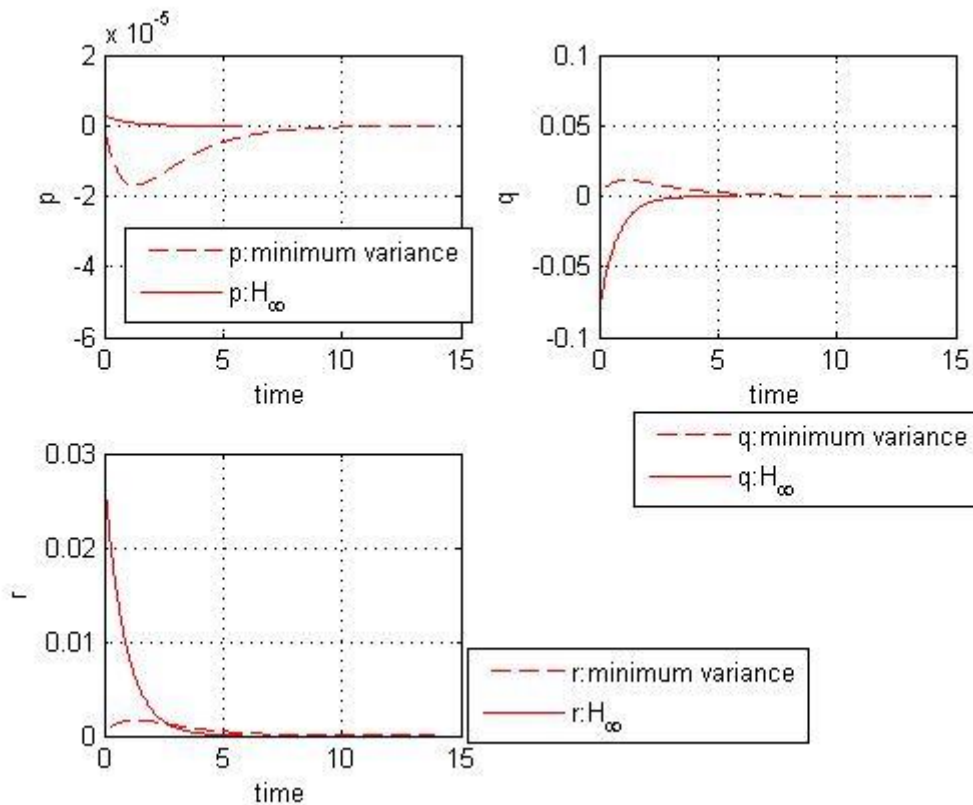


Figure 3.20 Comparison between the minimum variance and H infinity methods for roll p , pitch q and yaw r for the conditions given at examples 1 and 5

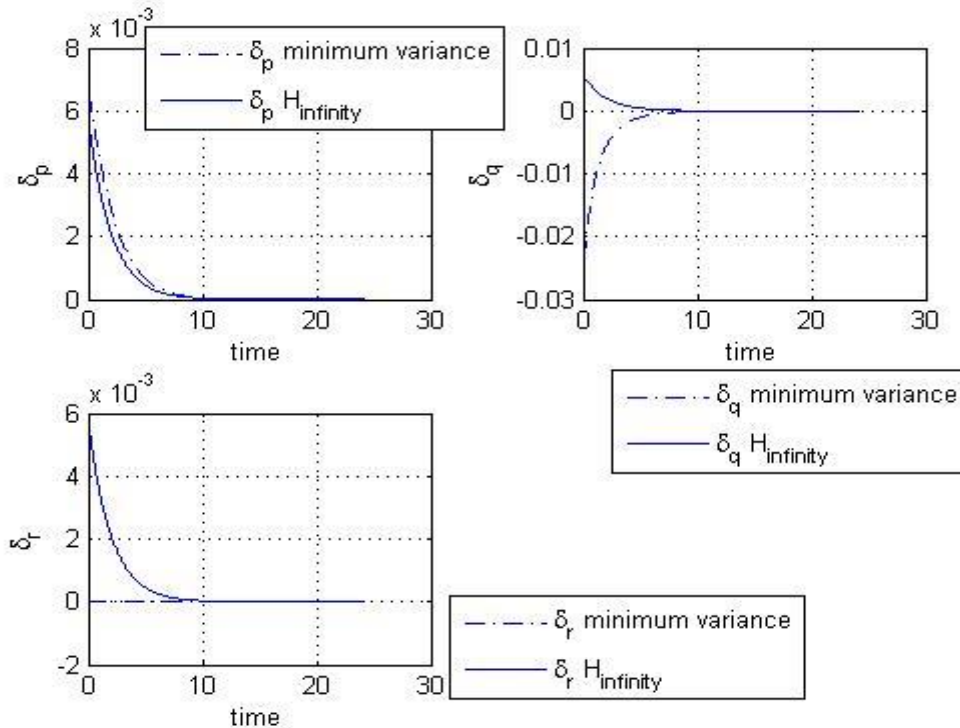


Figure 3.21 Comparison between the minimum variance and H infinity methods for the roll variation δ_p , the pitch variation δ_q and the yaw variation δ_r for the conditions given at examples 1 and 5.

From fig.3.19 to 3.21 one can see the comparison between example 1 and 5.

In fig.3.19 one can see that the angle of attack converges to zero faster in the H-infinity method then in the minimum variance and for the sideslip angle it is possible to see that the H-infinity controller will converge faster than the minimum variance controller.

In fig. 3.20 it is possible to see in the roll one that the minimum variance controller descends to -0.000005 radian per second and then rises back to zero in around 10 seconds while the H-infinity will stay near zero all the time in the pitch value it is possible to see that the minimum variance controller will rises to 0.001 radian per second and then stabilizes to zero while the H-infinity one will rises continuously to zero in around 3 seconds.

In figure 3.21 it is possible to that for the roll controller both methods give almost the same results, the pitch controller figure shows that while the minimum variance controller ascends to zero in around 10 seconds while the H-infinity will descend to zero in around ten seconds finally for the yaw controller while the minimum variance controller will stay at zero the H-infinity one will descends to zero in around 10 seconds.

The following set of figures shows the superposition between both methods for examples 2 and 6.

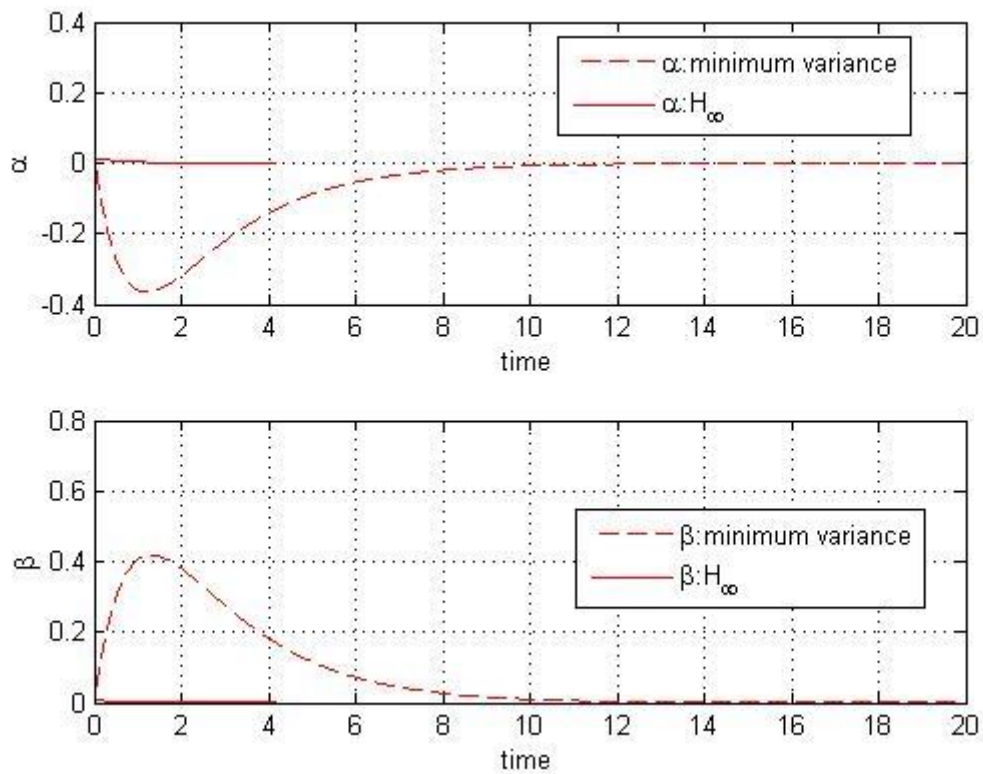


Figure 3.22 Comparison between the minimum variance and H infinity methods for the angle of attack α and the sideslip angle β for the conditions given at examples 2 and 6

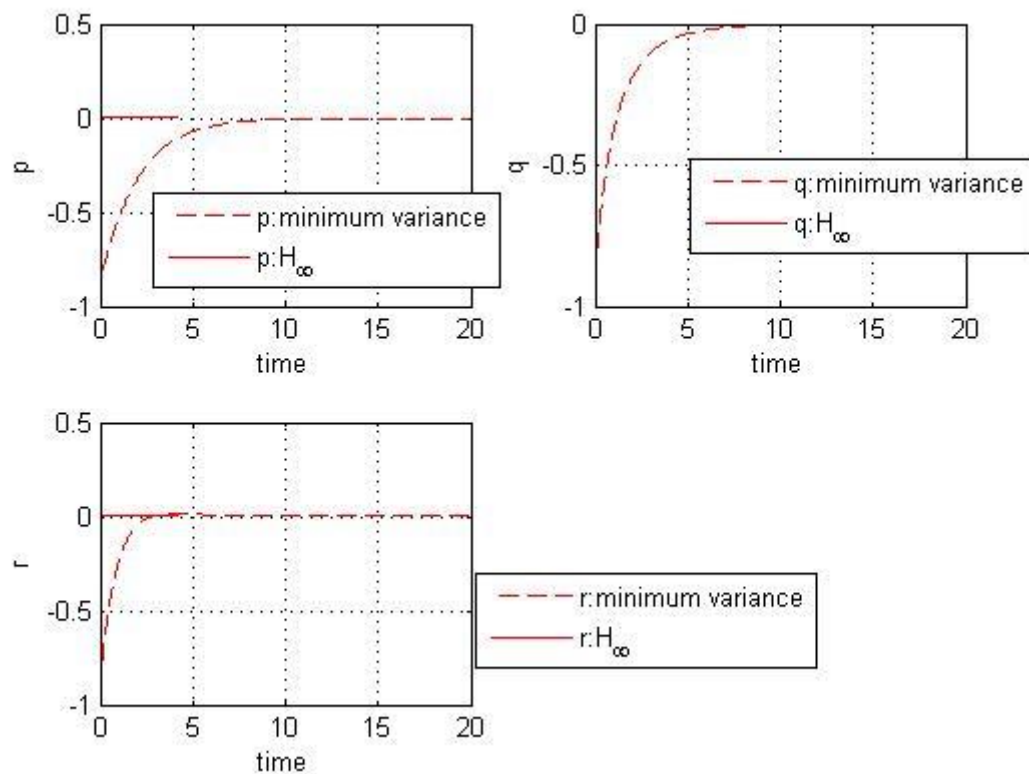


Figure 3.23 Comparison between the minimum variance and H infinity methods for roll p , pitch q and yaw r for the conditions given at examples 2 and 6

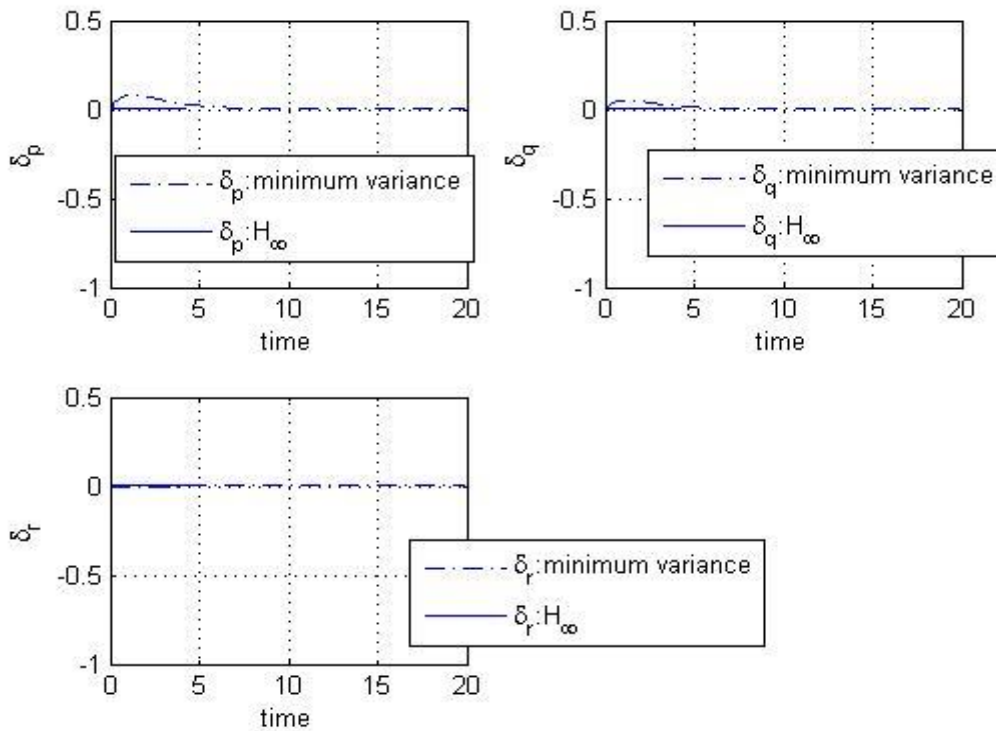


Figure 3.24 Comparison between the minimum variance and H infinity methods for the roll variation δ_p , the pitch variation δ_q and the yaw variation δ_r for the conditions given at examples 2 and 6

From fig.3.22 to 3.24 one can see the comparison between example 2 and 6.

In fig.3.22 one can see that the angle of attack in the H-infinity will almost immediately converge to zero while the minimum variance controller will descend to -0.035 radian per second and then rises to zero in around 10 seconds the same happens to the sideslip angle but the minimum variance controller is almost symmetric.

Fig. 3.23 it is possible to see in the all the graphics that while the H-infinity values stay at zero those of the minimum variance rises from nearly -0.7 radian per second to zero in around 10 seconds.

In figure 3.24 it is possible to that for all the graphics in this figure that both the controllers stay near zero in this experiment.

The following set of figures shows the superposition between both methods for examples 3 and 7

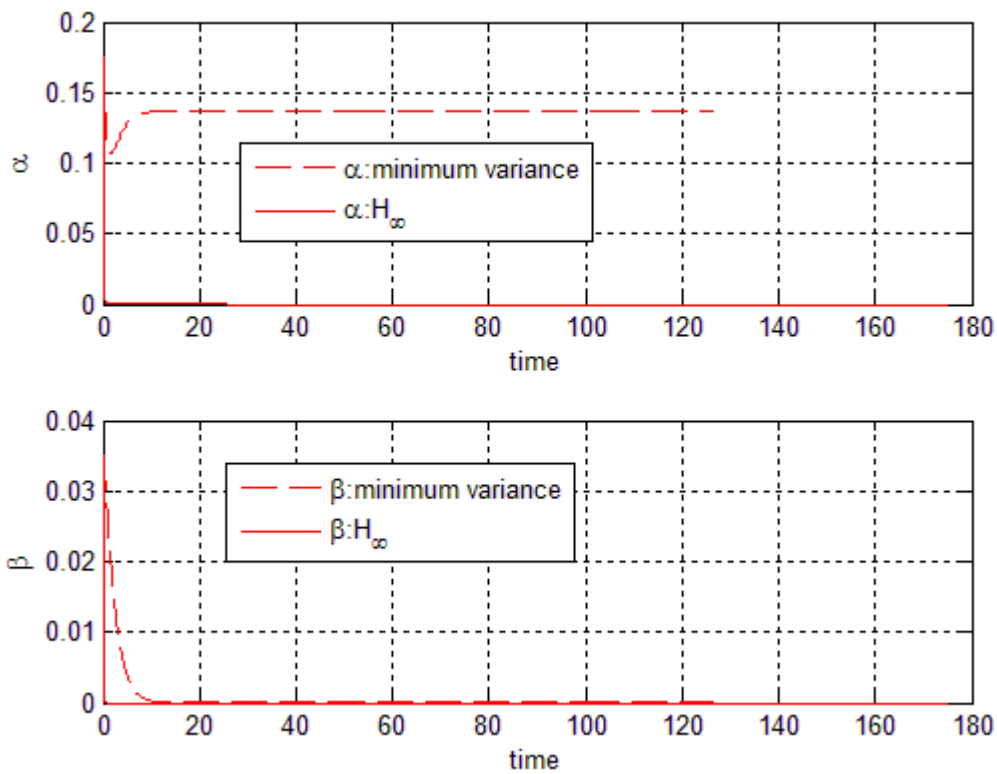


Figure 3.25 Comparison between the minimum variance and H infinity methods for the angle of attack α and the sideslip angle β for the conditions given at examples 3 and 7

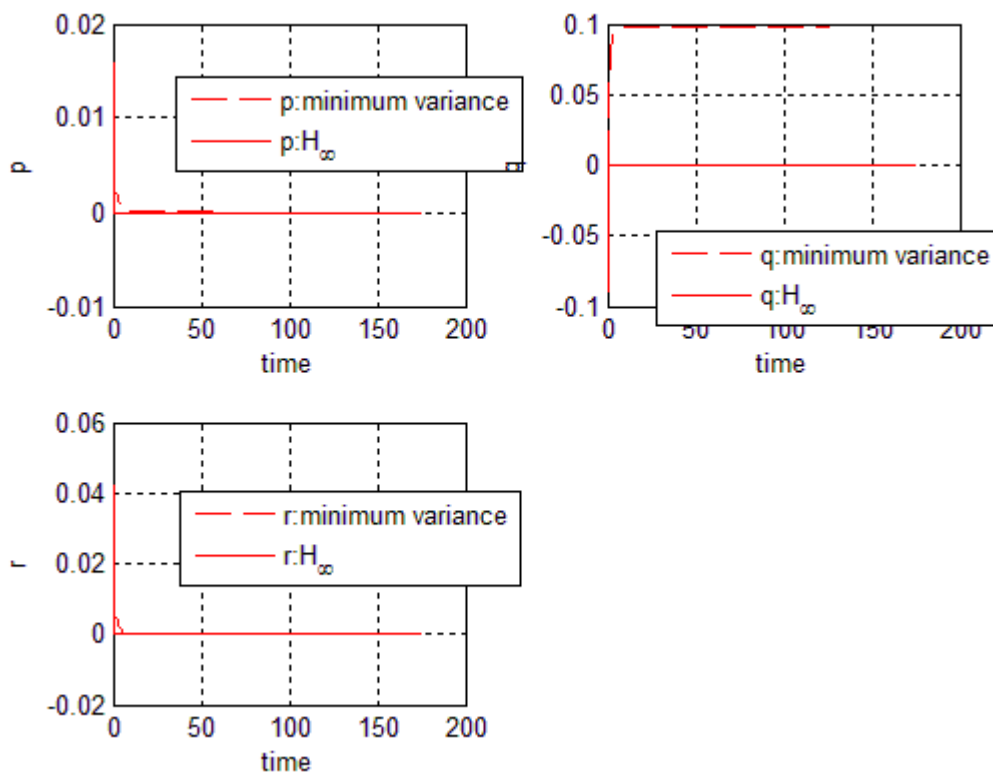


Figure 3.26 Comparison between the minimum variance and H infinity methods for roll p , pitch q and yaw r for the conditions given at examples 3 and 7

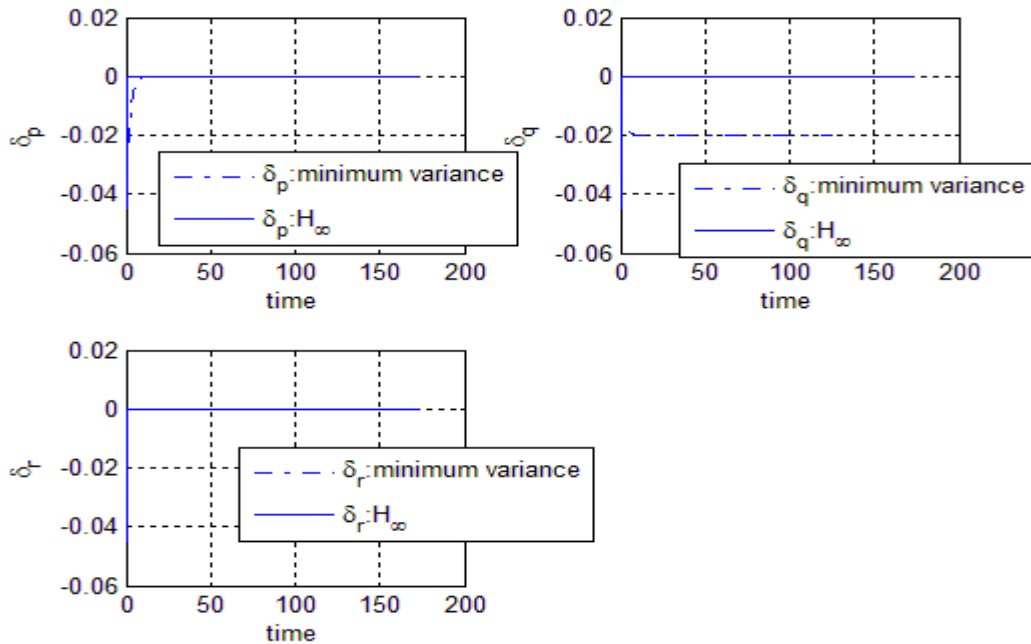


Figure 3.27 Comparison between the minimum variance and H infinity methods for the roll variation δ_p , the pitch variation δ_q and the yaw variation δ_r for the conditions given at examples 3 and 7.

From fig.3.25 to 3.27 one can see the comparison between example 3 and 7.

In fig.3.25 one can see that the angle of attack that while for the minimum variance the result is close to 0.15 radian per seconds for the H infinity it will tend to the proximity of zero almost immediately but will only reach in zero in 4 seconds, and for the sideslip angle it is possible to see that the minimum variance will tend to zero in nearly 10 seconds while the H-infinity tends to zero in nearly 4 seconds.

In fig. 3.26 it is possible to see that both the roll and the yaw that they are almost identical but in the pitch it is possible to see that where the H-infinity stays at zero the minimum variance controller will reach 0.1 radian per second.

In figure 3.27 it is possible to that for the roll and yaw controllers both methods give almost the same results as for the pitch controller that while the minimum variance controller tends for -0.02 radian per second H infinity tends for zero.

In all those sets of figures it is possible to see that the H-infinity gives better and faster results that the minimum variance but requires a higher time of processing and is very difficult to obtain in practice.

As for the times using the commands tic and toc in Matlab it is possible to see that for the minimum variance the time is around 3 seconds while for the H-infinity the time is around 11 seconds.

Another advantage of the minimum variance will be the fact that the flight model can change inflight while the H-infinity model is fixed.

Knowing this it is possible to state that even being a bit less fast to respond the minimum variance controller will be faster to compute, easier to obtain in practice and the model can change inflight if needed.

4. Conclusion

As described the objective of this work is to make a minimum variance controller for the lateral directional part of the flight of a missile so in order to reach this goal various methods were discussed and finally the minimum variance was chosen.

To reach the goal the method shown in chapter 3 was used in order to obtain a good representation of the real conditions experimented in a flight.

After the minimum variance simulation were run it is possible to conclude that for the first stability point used that for all points and in both the longitudinal and lateral-directional part of the flight and that stabilized in a short amount of time, for the second stability point it is possible to see that for the lateral-directional part of the flight the condition are stable but not the longitudinal which can be due to the fact that this stability point is not a Lyapunov point of stability.

For the H-infinity results it is possible to see that for both stability point all the tested points are stable both in the longitudinal and lateral-directional part of the flight and stabilizes rather quickly,

Analyzing both the methods results it is possible to see that the H-infinity method stabilizes faster than the minimum variance but requires much more computation effort, if we consider the time differences between the two methods the minimum variance method is the easiest to implement and the fastest to compute, as proven by the comparison and considering that in most of the tested points the H-infinity will almost immediately tend to zero this is impossible to obtain in practical terms.

As described earlier the minimum variance controller will compute faster, is easier to obtain in practice and can be changed inflight.

This work could be improved by making a more complete comparison between minimum variance and other methods like LQR.

In the H-infinity comparison more gains could have been tested in order to have better comparison between methods.

Another point where this work can be improved is to study the longitudinal part of the flight.

Also one other field of study will be to make an hybrid controller between H-infinity and minimum variance to take the advantages of both.

This work could be improved in the future by using nonlinear conditions and all of those improvements can in the future be practically tested.

An improvement to the minimum variance controller can be making it more robust so that noises will have a lesser influence on the control. And thus making the cross coupling less relevant.

5. References

- [1] Siouris, G.M. “*Missile Guidance and Control systems*”, Springer, Paris, 2004.
- [2] Wikipedia, www.wikipedia.com , last visit September 2013.
- [3] Reidel, F.W “*Bank-To-Turn Control Technology Survey for Homing Missiles*”, NASA Contractor Report 3325, 1980, pp 26.
- [4] Capt. Smith, J.S. USAF, “*An Autopilot Design Methodology for Bank-to-turn*” Missiles Guidance And Control Branch, Aeromechanics Division, AFATL-Tr-89-49, AD-A213 379, 1989. pp 11-47.
- [5] Yanushevsky,R., *Modern Missile Guidance*, CRC Press, London, 2008.
- [6] Khalil, H.K, *Nonlinear Systems*, Third Edition, Prentice Hall, Upper Saddle River N.J., 2002.
- [7] Gadewadikar, J, “*H-infinity output-feedback control: application to unmanned aerial vehicle*”, PhD Thesis University of Texas at Arlington, 2007.
- [8] Engwerda, J.C and Otter, P.W., “On the choice of weighting matrices in the minimum variance controller”, *Automatica*, Vol.25, No.2,1989, pp. 279-285.
- [9] Engwerda, J.C., “The solution of the infinite trajectory tracking problem for discrete time systems possessing an exogenous component” Memorandum Cosor 86-08 Eindoven University of Technology, 1986.
- [10] Carter, L.H., and. Shamma, J.S. “Gain-Scheduled Bank-to-Turn Autopilot Design Using Linear Parameter Varying Transformations”, *Journal of Guidance, Control, and Dynamics*, vol. 19, no. 5 , September-October, 1996, pp 1056-1063.

6. Annex A (Publication)

Minimum Variance Lateral-Directional Control of a Bank-to-Turn Missile

D. Medroa, K. Bousson
LAETA-UBI/AeroG
Department of Aerospace Sciences
University of Beira Interior
6200-001 Covilhã - Portugal

Abstract. In this work a Bank-To-Turn (BTT) lateral directional controller was made using a minimum variance method described later. It was compared with an H-infinity controller. In order to see first of all if the system converges and how it compares to another method. The models were analyzed using the state and control equations like the angle of attack, the sideslip angle, the roll, the pitch, the yaw, the roll controller, the pitch controller and the yaw controller.

List of variables

p = roll

q = pitch

r = yaw

C_l, C_m, C_n = aerodynamic moment coefficients about body x, y and z axes respectively

C_x, C_y, C_z = aerodynamic force coefficients along body x, y, z axes respectively

d = missile reference diameter

$I_{xx}, I_{yy}, I_{zz}, I_{xz}$ = moments of inertia about body

$I_1 - I_5$ = Constants dependent on moments of inertia

K_Q = constant dependent on flight condition

Q = dynamic pressure

S = reference area

u = controller input

α = angle of attack

β = angle of sideslip

δ_p = roll control deflection

δ_q = pitch control deflection

δ_r = yaw control deflection

P = Riccati equation solution

A = System matrix

B = Control matrix

C = Output matrix

D = Disturbance matrix

K = Gain matrix

I. Introduction

First of all let's define BTT or Bank-to-turn, it is no more than a way of turning a missile orienting the maximum of aerodynamic normal force with the plane of the commanded direction using the pitch and roll movement while maintaining a very small sideslip angle.

The reason why BTT was used in this work, is the fact that comparing with others like Skid-To-Turn (STT) he offers a best rang for the same amount of fuel, a much larger acceleration in the maneuver plan, a better aerodynamic efficiency and allows to have biggest g forces in at the final part of the flight for this reason it might be used in short, mid and long air to air strikes as well as in air to surface missiles as seen in [1].

After this brief explication of BTT the minimum variance controller will be defined as follow it consists in predicting the system in the next used time in order to control the system in the present time and seeks a control that minimizes a determinate performance function that for this work will be given in the next chapter. The advantages of this type of controllers are simpler to implement and just as fast as other methods offering a good stability for linearized models thus allowing to minimize the cross coupling problem of a latero directional BTT model one of the BTT biggest inconvenient not compromising speed. Therefore this is the reason why a minimum variance controller is used in this work.

II. Control models

II.1. Minimum Variance control model

According to [2] it is possible to consider the following linear finite dimensional difference equation

$$y(k+1) = Ay(k) + Bu(k) + c(k) + v(k) \quad (1)$$

where $y(k)$ is a n-dimensional output/target vector observed in period k ; $u(k)$ is a m-dimensional input/control vector with $m \leq n$; $c(k)$ is a p-dimensional deterministic input, called exogenous input and is assumed to be known at period k ; $v(k)$ is a serially uncorrelated vector with zero mean and covariance V(white noise), Assuming that matrix B is injective(full column rank) and that the pair (A,B) is controllable.

Considering the cost functional equation

$$J = E \left\{ \left(y(k) - y^*(k) \right)^T P \left(y(k) - y^*(k) \right) \right\} \quad (2)$$

where $E\{\cdot\}$ denotes the expectation $y^*(k)$ is a reference value for $y(k)$ and Q is symmetric positive definite weighting matrix. Assuming that the reference trajectory is given by the first order difference equation

$$y^*(k+1) = A^* y^*(k) \quad (3)$$

knowing $y^*(0)$ and A^* .

Subtracting equations (3) from (1) yields

$$e(k+1) = Ae(k) + Bu(k) + x(k) + v(k) \quad (4)$$

where

$$e(k) = y(k) - y^*(k) \quad (5)$$

And

$$x(k) = (A - A^*)y^*(k) + v(k) \quad (6)$$

the optimal control minimizing J subject to the last equation is given by straight forwarding differentiation and equals

$$u(k) = -(B^T PB)^{-1} B^T P(Ae(k) + x(k)) \quad (7)$$

II.2 H-Infinity control model

First of all a brief description of the H-infinity theory will now be made according to [3]. If one consider the following system

$$\begin{aligned} \dot{x} &= Ax + Bu + Dd \\ y &= Cx \end{aligned} \quad (14)$$

And a performance output z(t) that satisfies

$$\|z(t)\|^2 = x^T Qx + u^T Ru \quad (15)$$

For some positives matrices $Q \geq 0$ and $R > 0$. Assuming C has a full row rank. Considering a L_2 system it's gain is said to be bounded or attenuated by γ if

$$\frac{\int_0^{\infty} \|z(t)\|^2 dt}{\int_0^{\infty} \|d(t)\|^2 dt} = \frac{\int_0^{\infty} (x^T Qx + u^T Ru) dt}{\int_0^{\infty} (d^T d) dt} \leq \gamma^2 \quad (16)$$

It is possible to define a constant output-feedback control as

$$u = -Ky = -KCx \quad (17)$$

It is desired to find a constant output-feedback gain K such that the system is stable.

If one assume that $Q \geq 0$ and (A, \sqrt{Q}) is detectable then the output-feedback is stabilizable with L_2 gain bounded by γ if (A, B) is stabilizable and (A, C) is detectable and there exists matrices K^* and L such that $K^* C = R^{-1}(B^T P + L)$ where $P > 0$, $P^T = P$ is a solution of

$$PA + PA^T + Q + \frac{1}{\gamma^2} PDD^T P - PBR^{-1}B^T P + LR^{-1}L = 0 \quad (19)$$

II.3 Missile model

Using [4] a BTT missile is nearly symmetrical in the pitch plane, two of the three cross products of inertia (I_{xy}, I_{yz}) are assumed to be zero, with these assumptions the missile dynamics are given as follows:

$$\begin{aligned} \dot{\alpha} &= K_Q [-C_x \sin a + C_x \cos a] - \tan \beta (\rho \cos a + r \sin a) + q \\ \dot{\beta} &= K_Q [C_y \cos \beta - C_x \cos a \sin \beta - C_x \sin a \sin \beta] - r \cos a - p \sin a \\ \dot{p} &= I_1 pq + I_2 QSdC_l + I_3 QSdC_n \\ \dot{q} &= \left(\frac{I}{I_{yy}} \right) [I_{xz} (r^2 - p^2) + (I_{zz} + I_{xx}) pr + QSdC_m] \\ \dot{r} &= I_4 pq + I_3 QSdC_l + I_5 QSdC_n \end{aligned} \quad (29)$$

Note that the preceding equations exhibit significant explicit kinematic and inertial coupling and implicit through the aero coefficients. Specifically a BTT missile will develop a large roll rate and angle of attack while maintaining a very small sideslip angle. Therefore, the roll rate will require a large yaw rate to maintain that very small sideslip.

The controls appear in the aerodynamic force and moment coefficients, which in general are complicated nonlinear functions of both the states and controls. These are in the form of tabular data and so functional approximations were created by curve fitting the resulting aerodynamic model is as follows

$$\begin{aligned} C_x(\alpha) &= C_{x0} + C_{x\alpha} \alpha \\ C_y(\beta, \delta_r) &= C_{y\beta} \beta + C_{y\delta_r} \delta_r \\ C_z(\alpha, \delta_q) &= C_{z0} + C_{z\alpha} \alpha + C_{z\delta_q} \delta_q \\ C_l(\alpha, \beta, \delta_p, \delta_r) &= (a_1 + a_2 \alpha) \beta + C_{l\delta_p} \delta_p + a_3 a \delta_r \\ C_m(\alpha, \delta_q) &= C_{m0} + C_{m\alpha} \alpha + C_{m\delta_q} \delta_q \\ C_n(\delta_r) &= C_{n\delta_r} \delta_r \end{aligned} \quad (30)$$

The guidance commands for a BTT airframe may require a large angle of attack and roll rate, while minimizing the sideslip angle. When both the angle of attack and roll rate become large the dynamic cross coupling nonlinearities become most evident.

As previously noted, the missile dynamics are highly coupled and nonlinear, a high roll rate and angle of attack induce a high yaw rate and pitch/yaw/roll kinematic coupling according to [4].

III. Simulation data

In this work the stability point used was $\alpha = 0, \beta = 0, p = 0, q = 0, r = 0$.

In this point the missile equations were linearized and the matrix A and B resultant of that linearization are given as follow

$$A = \begin{bmatrix} -0.9067 & 0 & 0 & 1 & 0 \\ -0 & -0.3601 & 0 & 0 & -1 \\ 0 & 519.1597 & 0 & 0 & 0 \\ -31.9490 & 0 & 0 & 0 & 0 \\ 0 & -5.1746 & 0 & 0 & 0 \end{bmatrix} \quad (31)$$

$$B = \begin{bmatrix} 0 & -0.2 & 0 \\ 0 & 0 & 0.2 \\ -2690.9 & 0 & 124.3 \\ 0 & -219.9 & 0 \\ 26.8 & 0 & -192.3 \end{bmatrix} \quad (32)$$

III.1 Minimum variance data

Since a minimum variance controller was used and that they are discrete these matrices were discretized and the result is given as follow

$$A_d = \begin{bmatrix} 0.9894 & 0 & 0 & 0.0100 & 0 \\ 0 & 0.9967 & 0 & 0 & -0.0100 \\ 0 & 5.1822 & 1 & 0 & -0.0260 \\ -0.3180 & 0 & 0 & 0.9984 & 0 \\ 0 & -0.0517 & 0 & 0 & 1.0003 \end{bmatrix} \quad (33)$$

$$B_d = \begin{bmatrix} 0 & -0.0128 & 0 \\ -0.0013 & 0 & 0.0112 \\ -26.9109 & 0 & 1.2642 \\ 0 & -2.1976 & 0 \\ 0.2682 & 0 & -1.9236 \end{bmatrix} \quad (34)$$

Using a discrete LQR controller the weighting matrix was obtained and is given as follow

$$P = \begin{bmatrix} 46.5710 & 0 & 0 & 0.2037 & 0 \\ 0 & 72.8544 & 0.0057 & 0 & 0.4560 \\ 0 & 0.0057 & 1.0014 & 0 & 0.0030 \\ 0.2037 & 0 & 0 & 1.1770 & 0 \\ 0 & -0.4560 & 0.0030 & 0 & 1.2271 \end{bmatrix} \quad (35)$$

And given the positivity of this matrix the point will be stable.

Since the matrices A_d , B_d and P were obtained it is now possible to simulate this controller.

III.2 H-infinity data

After the linearization we need to obtain the gain, using [5] the first step will be to solve the following equation to obtain the gain,

$$PA + PA^T + Q + \frac{1}{\gamma^2} PDD^T P - PBR^{-1}B^T P + LR^{-1}L = 0 \quad (22)$$

Since C is an identity matrix then L will be 0, $Q = C^T C$ and since disturbance was used D is given as follow

$$D = \begin{bmatrix} 0 & 0 \\ 0 & 0.1 \\ 0.1 & 0 \\ 0 & 0 \\ 0 & 0 \end{bmatrix} \quad (22)$$

Since P will be obtained using a Riccati equation the following equations will be used

$$PA + PA^T + P(\gamma^{-2}DD^T - BB^T)P + Q = 0 \quad (23)$$

After rewriting the last equation in the Riccati equation form one obtain the following equation

$$PA + PA^T + P\bar{B}\bar{R}\bar{B}^T P + Q = 0 \quad (24)$$

Where \bar{B} is given by $[D, B]$,

$$R = \begin{bmatrix} -0.0441 & 0 & 0 & 0 & 0 \\ 0 & -0.0441 & 0 & 0 & 0 \\ 0 & 0 & 1 & 0 & 0 \\ 0 & 0 & 0 & 1 & 0 \\ 0 & 0 & 0 & 0 & 1 \end{bmatrix} \quad (25)$$

After solving the Riccati equation the matrix is obtain and given as follow

$$P = \begin{bmatrix} 0.5220 & 0 & 0 & 0.0013 & 0 \\ 0 & 1.3587 & -0.0005 & 0 & -0.0047 \\ 0 & -0.0005 & 0.0004 & 0 & 0 \\ 0.0013 & 0 & 0 & 0.0046 & 0 \\ 0 & -0.0047 & 0 & 0 & 0.0053 \end{bmatrix} \quad (26)$$

The gain will be given by the following equation

$$K = R^{-1}(B^T P + L) \quad (27)$$

And in this conditions the gain is

$$K = \begin{bmatrix} 0 & -0.0017 & -0.01 & 0 & -0.0003 \\ -0.0031 & 0 & 0 & -0.0100 & 0 \\ 0 & 0.0078 & 0.0003 & 0 & -0.01 \end{bmatrix} \quad (28)$$

IV. Simulation results

In order to test if the system an initial point was chose, the point is $\alpha = 10^\circ$, $\beta = 2^\circ$, $p = 0$, $q = 0$, $r = 0$, $\delta_p = 10^\circ$, $\delta_q = 20^\circ$, $\delta_r = 8^\circ$

And the results are shown in the following figures

State Conditions figures:

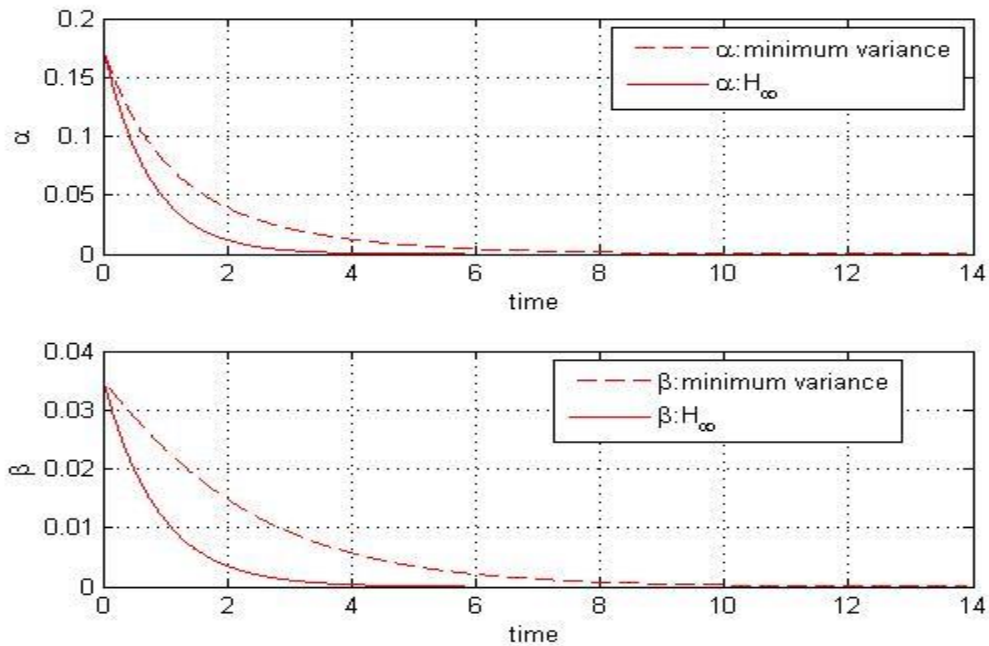


Figure 1- variation of the angle of attack alpha in radian per second with time in the analyzed conditions and the sideslip angle beta in radian per second with time in the analyzed conditions

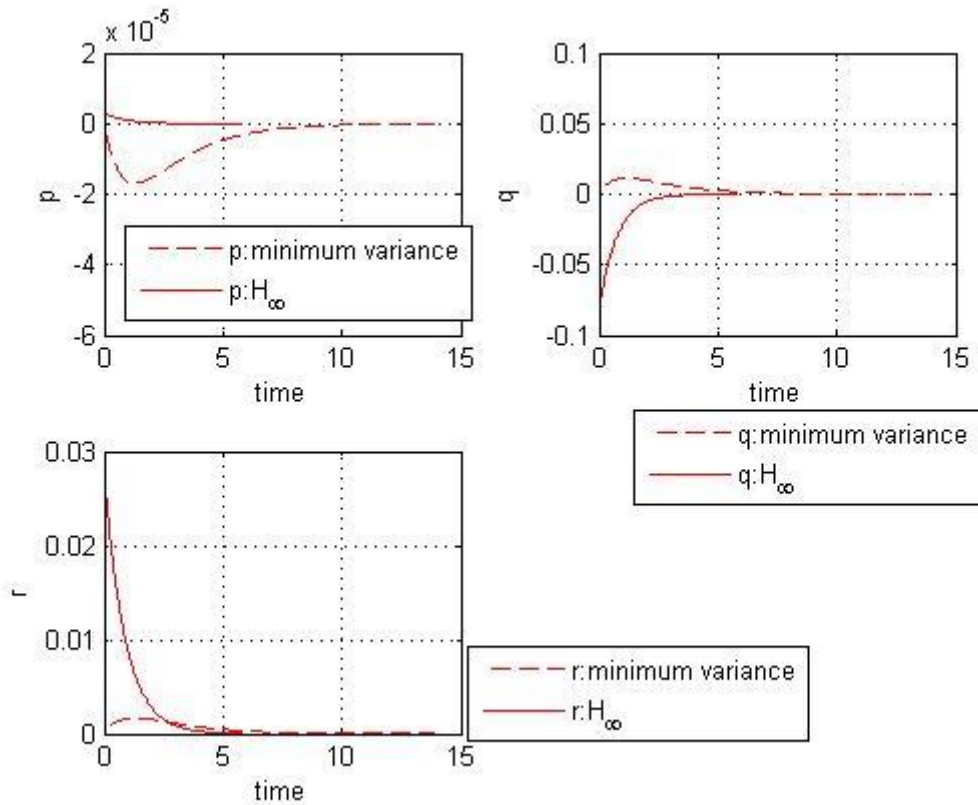


Figure 2- variation of roll p in radian per second with time for the analyzed conditions, variation of pitch q in radian per second with time for the analyzed conditions and the variation of yaw r in radian per second with time for the analyzed conditions.

Controllers figure:

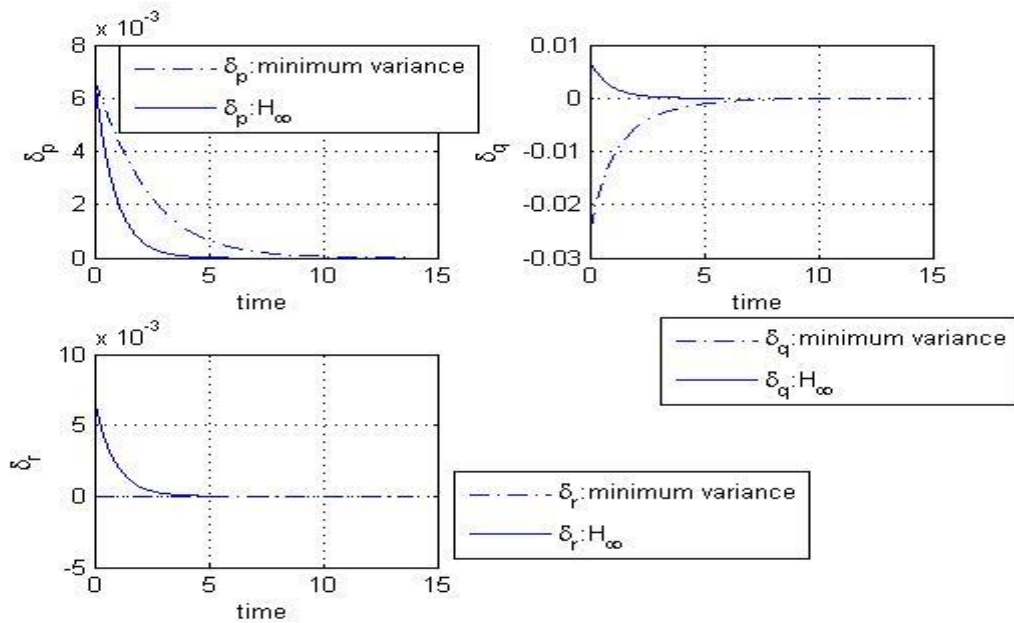


Figure 3- variation of the roll controller δ_p in radian per second with time for the analyzed conditions, the pitch controller δ_q in radian per second with time for the analyzed conditions and the yaw controller δ_r in radian per second with time for the analyzed conditions.

After running these simulation the following observations can be made:

First of all the state conditions will be stabilized by the tested controller since all the figures will tend to the reference point for both the methods.

figure 1 shows that for the angle of attack it is possible to see that both the methods tends to zero the H-infinity will tend faster around 4 seconds than the minimum variance one that will tend in 10 seconds, for the sideslip angle they while both tend to zero the H-infinity controller tends to zero in 4 seconds the minimum variance tends to zero in 10 seconds.

In figure 2 it is possible to see that the roll p stays close to zero for all the duration of the experiment in the H-infinity while in the minimum variance it will reach -0.00005 radian per second and then reach zero in 10 seconds, the pitch q stays close to zero for the minimum variance controller while in the H-infinity controller it will rise from -0.055 radian per second to zero in around 5 seconds and finally it is possible to see that for the yaw it stays near zero for all the analysis for the minimum variance controller and that for the H-infinity one it descends continuously to zero in around 4 seconds.

In figure 3 it is possible to see that for the roll controller both the methods will tend to zero the H-infinity will reach zero in around 4 seconds the minimum variance method will reach zero in 10 seconds, for the pitch controller it is possible to see that the H-infinity controller reaches zero in around 5 seconds from almost 0.01 radian per second, the minimum variance controller will reach 0 in around 10 seconds starting from -0.02 radian per second and finally it is possible to see that the yaw controller stays around zero for the entire analysis in the minimum variance controller while descending from nearly 0.005 radian per second and will reach zero in around 5 seconds.

V. conclusion

After running this analysis it is possible to conclude that despites converging faster the H-infinity have a slower computation and requires more computation power while the minimum variance method converge a bit slower but is much faster to compute and easier to use and as such a good way of controlling BTT missiles. This work could be improved by comparing it not only to an H-infinity controller but also to a LQR controller. Another point of improvement could be making the Minimum variance controller more robust so the controller is less sensible to noises and cross coupling.

VI. missile data

Mach=2.75; Altitude= 40000 ft; Q=2073,7 lb ft⁻²; $K_Q = 0.0339s^{-1}$; $I_{xx} = 1.0798$; $I_{xz} = 70.131$;

$$I_{zz} = 70.6609; \quad I_{yy} = -0.7043; \quad I_1 = \frac{I_{xx}I_{xz} + I_{xz}(I_{xx} - I_{yy})}{I_{xx}I_{zz} - I_{xz}^2}; \quad I_2 = \frac{I_{zz}}{I_{xx}I_{zz} - I_{xz}^2};$$

$$I_3 = \frac{I_{xz}}{I_{xx}I_{zz} - I_{xz}^2}; \quad I_4 = \frac{I_{xz}^2 + I_{xx}(I_{xx} - I_{yy})}{I_{xx}I_{zz} - I_{xz}^2}; \quad I_5 = \frac{I_{xx}}{I_{xx}I_{zz} - I_{xz}^2}; \quad \text{Weight}=227 \text{ lb}; \quad S= 0.3068 \text{ ft}^2;$$

D=7.5 in; $C_{x0} = -0.4962$; $C_{x\alpha} = 0.1699$; $C_{y\beta} = -11.1180$; $C_{y\delta r} = 4.6346$; $C_{z\omega} = -0.1006$;

$C_{z\alpha} = -27.2417$; $C_{z\delta q} = -5.4832$; $a_1 = 1.4008$; $a_2 = -25.7771$; $a_3 = -4.4423$;

$C_{l\delta p} = -7.2605$; $C_{m0} = -1.4785$; $C_{m\alpha} = -5.6355$; $C_{m\delta q} = -38.7896$; $C_{n\delta r} = -33.6611$

VII. references

- [1] Capt. Smith, J.S. USAF, "An Autopilot Design Methodology for Bank-to-turn" Missiles Guidance And Control Branch, Aeromechanics Division, AFATL-Tr-89-49, AD-A213 379, 1989. pp 11-47.
- [2] Engwerda, J.C and Otter, P.W., "On the choice of weighting matrices in the minimum variance controller", *Automatica*, Vol.25, No.2,1989, pp. 279-285.
- [3] Gadewadikar, J, "H-infinity output-feedback control: application to unmanned aerial vehicle", PhD Thesis University of Texas at Arlington, 2007.
- [4] Carter, L.H., and Shamma, J.S. "Gain-Scheduled Bank-to-Turn Autopilot Design Using Linear Parameter Varying Transformations", *Journal of Guidance, Control, and Dynamics*, vol. 19, no. 5 , September-October, 1996, pp 1056-1063.

